Region II Storm Surge Project – Spatially Varying Nodal Attribute Parameters

September 2014

FEMA

Federal Emergency Management Agency
Department of Homeland Security
500 C Street, SW
Washington DC, 20472

Contract: HSFEHQ-09-D-0369
Task Order: HSFE02-09-J-0001

This document was prepared by

RAMPP
8401 Arlington Blvd.
Fairfax, VA 22031

TABLE OF CONTENTS

Figures

Tables

Appendices

ADCIRC	ADvanced CIRCulation Model for Oceanic, Coastal and Estuarine Waters
CTP	Cooperating Technical Partner
FEMA	Federal Emergency Management Agency
GAP	Gap Analysis Program
GIS	Geographical Information Systems
NJDEP	New Jersey Department of Environmental Protection
NJLU	New Jersey Land Use/Land Cover
NLCD	National Land Cover Dataset
NOAA	National Oceanic and Atmospheric Administration
SWAN	Simulating WAves Nearshore Model
SWEL	Stillwater Elevation
UnSWAN	Unstructured Simulating Waves Nearshore Model

SECTION ONE INTRODUCTION

The Federal Emergency Management Agency (FEMA) contracted Risk Assessment, Mapping, and Planning Partners (RAMPP), a joint venture of Dewberry, URS, and ESP, under its Risk Mapping, Assessment, and Planning (Risk MAP) program to provide comprehensive floodplain mapping, Geographic Information System (GIS), and hazard risk mitigation services. This report summarizes the methodology used to develop one of the input files to the storm surge model which was used for part of the coastal hazard analysis to support Flood Insurance Studies (FIS) in Region II.

The ADvanced CIRCulation (ADCIRC) model for Oceanic, Coastal and Estuarine Waters allows incorporation of an additional input file called the nodal attributes file (or fort.13 file). This input file lets the user specify model parameters on a node-by-node basis to allow spatial variation in the parameter values. For the Region II storm surge study, the following parameters were used:

- Manning's n at sea floor,
- surface directional effective roughness length,
- surface canopy coefficient,
- wave refraction in the Unstructured Simulating WAves Nearshore (UnSWAN) model, and
- primitive weighting in continuity equation parameters.

Several Fortran codes, developed for the North Carolina storm surge study and available on the ADCIRC website (http://adcirc.org/home/related-software/adcirc-utility-programs/), were the basis for some of the nodal attributes file created for the Region II storm surge study, but some parameters were changed, as discussed below. Three of the nodal attributes were dependent on land use data; therefore, the selection of the land use data is described before the description of the nodal attribute parameters.

SECTION TWO LAND USE DATA SOURCES

Land use data is the basis for the definition of the *Manning's n at sea floor, surface canopy coefficient,* and *surface directional effective roughness length* parameters. Three sources of land use data are available for various parts of the project area. These datasets are the National Land Cover Dataset (NLCD), Gap Analysis Program (GAP) dataset, and the New Jersey Land Use (NJLU) dataset. The use of different datasets can result in differences in the parameters listed above. Therefore, the land use datasets were examined to determine the best land use data for the Region II storm surge study. The sections below describe the selection process and the final dataset.

2.1 LAND USE DATASET DATES

The NLCD data was developed in 2001. The GAP data were combined from datasets generated from 1999 through 2001. The NJLU data were updated in 2007 from previous versions generated in 2002, 1995, and 1986. Both the NLCD and GAP data were in raster format. The NJLU dataset is a shapefile consisting of many polygons.

2.2 LAND USE DATASET CLASSIFICATIONS

For New Jersey and New York, the NLCD dataset consists of 16 classifications, the GAP dataset contains 53 classifications at the finest level of detail, and the NJLU dataset contains 90 classifications at the finest level of detail. The large discrepancy in numbers of classes could be misleading, as the finest level of detail for the GAP and NJLU datasets contains redundant classes for the purposes of determining the nodal attribute parameters. For example, the NLCD land cover codes have 1 class of deciduous forest, while the GAP dataset has more than 10 classes, and the NJLU dataset has 4 classes. Looking at the Manning's n parameter, because these redundant classes are grouped under the same Manning's *n* value, the classes do not necessarily increase the quality of the dataset. The classification codes and land cover descriptions of classes found in this region for the NLCD, GAP, and NJLU datasets are listed in Tables 1 through 3.

Table 1. Classification codes and land cover descriptions for NLCD data

NLCD Code	Land Cover Description
11	Open Water
12	Perennial Snow/Ice
21	Developed, Open Space
22	Developed, Low Intensity
23	Developed, Medium Intensity
24	Developed, High Intensity
31	Barren Land
41	Deciduous Forest
42	Evergreen Forest
43	Mixed Forest
52	Shrub/Scrub
71	Herbaceous
81	Hay/Pasture
82	Cultivated Crops
90	Woody Wetlands
95	Emergent Herbaceous Wetlands

Table 2. Classification codes and land cover for GAP data

GAP Code	Land Cover Description	GAP Code	Land Cover Description	GAP Code	Land Cover Description
1201	Developed, Open Space	4113	Laurentian-Acadian Northern Hardwoods Forest	5807	Northern Atlantic Coastal Plain Heathland and Grassland
1202	Developed, Low Intensity	4114	Northeastern Interior Dry – Mesic Oak Forest	7503	Atlantic Coastal Plain Southern Dune and Maritime Grassland
1203	Developed, Medium Intensity	4133	Atlantic Coastal Plain Dry and Dry-Mesic Oak Forest	7507	Northern Atlantic Coastal Plain Dune and Swale
1204	Developed, High Intensity	4211	Atlantic Coastal Plain Northern Maritime Forest	8102	Disturbed/Successional-Shrub Regeneration
1301	Quarries, Mines, Gravel Pits, Oil Wells	4313	Northern Atlantic Coastal Plain Dry Hardwood Forest	8103	Disturbed/Successional-Grass/Forb Regeneration
1402	Cultivated Cropland	4323	Laurentian-Acadian Northern Pine-(Oak) Forest	8107	Harvested Forest-Shrub Regeneration
1403	Pasture/Hay	4327	Laurentian-Acadian Pine-Hemlock-Hardwood Forest	8108	Harvested Forest-Grass/Forb Regeneration
2102	Open Water (Fresh)	4330	Central Appalachian Oak and Pine Forest	8202	Evergreen Plantation or Managed Pine
2103	Open Water (Brackish/Salt)	4331	Appalachian Hemlock-Hardwood Forest	8203	Managed Tree Plantation
3105	Undifferentiated Barren Land	4333	Acadian Low-Elevation Spruce-Fir-Hardwood Forest	8401	Introduced Upland Vegetation-Treed
3106	Atlantic Coastal Plain Northern Sandy Beach	4335	Central Appalachian Pine-Oak Rocky Woodland	8406	Introduced Riparian and Wetland Vegetation
3110	Unconsolidated Shore	4539	Northeastern Interior Pine Barrens	8501	Disturbed, Non-specific
3112	Northern Atlantic Coastal Plain Sandy Beach	4540	North Atlantic Coastal Plain Pitch Pine Barrens	8504	Ruderal Wetland and Forest
4104	Northeastern Interior Dry Oak Forest – Hardwood Modifier	4551	Acadian-Appalachian Montane Spruce-Fir Forest	9101	Acadian Salt Marsh and Estuary Systems
9109	Atlantic Coastal Plain Northern Tidal Salt Marsh	9224	Laurentian-Acadian Shrub-Herbaceous Wetland Systems	9803	Central Appalachian Riparian-Forest Modifier
9202	Southern Coastal Plain Non-riverine Basin Swamp-Okefenokee Bay/Gum Modifier	9233	Atlantic Coastal Plain Northern Fresh and Oligohaline Tidal Marsh	9818	Central Interior and Appalachian Floodplain Systems
9212	Central Interior and Appalachian Swamp Systems	9235	Atlantic Coastal Plain Northern Tidal Wooded Swamp	9819	Central Interior and Appalachian Riparian Systems

GAP Code	Land Cover Description	GAP Code	Land Cover Description	GAP Code	Land Cover Description
9213	Gulf and Atlantic Coastal Plain Swamp Systems	9240	Northern Atlantic Coastal Plain Basin Swamp and Wet Hardwood Forest	9820	Laurentian-Acadian Floodplain Systems
9214	Laurentian-Acadian Swamp Systems	9308	Laurentian-Acadian Alkaline Conifer-Hardwood Swamp	9843	Atlantic Coastal Plain Small Blackwater River Floodplain Forest
9220	Gulf and Atlantic Coastal Plain Tidal Marsh Systems	9501	Boreal Acidic Peatland Systems	9914	North-Central Interior Wet Flatwoods

Table 3. Classification codes and land cover descriptions for NJLU data

NJLU Code	Land Cover Description	NJLU Code	Land Cover Description	NJLU Code	Land Cover Description
1110	Residential, High Density, or Multiple Dwelling	1150	Mixed Residential	1300	Industrial
1120	Residential, Single-Unit Medium Density	1200	Commercial and Services	1400	Transportation/Communication/ Utilities
1130	Residential, Single-Unit Low Density	1211	Military Installations	1410	Major Roadway
1140	Residential, Rural Single Unit	1214	Former Military; Indeterminate Use	1411	Mixed Transportation Corridor Overlap Areas
1419	Bridge Over Water	1800	Recreational Land	4230	Plantation
1420	Railroad Facilities	1804	Athletic Fields (Schools)	4311	Mixed Forest (>50% Coniferous with 10–50% Crown Closure)
1440	Airport Facilities	1810	Stadium, Theaters, Cultural Centers, and Zoos	4312	Mixed Forest (>50% Coniferous with >50% Crown Closure)
1461	Wetland Rights-of-Way	1850	Managed Wetland, in Built-up, Maintained Rec Area	4321	Mixed Forest (>50% Deciduous with 10–50% Crown Closure)
1462	Upland Rights-of-Way, Developed	2100	Cropland and Pastureland	4322	Mixed Forest (>50% Deciduous with >50% Crown Closure)
1463	Upland Rights-of-Way, Undeveloped	2140	Agricultural Wetlands (Cranberry Farms and Modified Uplands)	4410	Old Field (<25% Brush Covered)
1499	Stormwater Basin	2150	Former Agricultural Wetlands (becoming shrubby, not built-up)	4411	Phragmites Dominate Old Field
1500	Industrial and Commercial Complexes	2200	Orchards, Vineyards, Nurseries, Horticultural Areas, Sod Farms	4420	Deciduous Brush/Shrub land

NJLU Code	Land Cover Description	NJLU Code	Land Cover Description	NJLU Code	Land Cover Description
1600	Mixed Urban or Built-up Land	2300	Confined Feeding Operations	4430	Coniferous Brush/Shrub land
1700	Other Urban or Built-up Land	2400	Other Agriculture	4440	Mixed Deciduous/Coniferous Brush/Shrub land
1710	Cemetery	4110	Deciduous Forest (10–50% Crown Closure)	4500	Severe Burned Upland Vegetation
1711	Cemetery on Wetland	4120	Deciduous Forest (>50% Crown Closure)	5100	Streams and Canals
1741	Phragmites Dominate Urban Area	4210	Coniferous Forest (10–50% Crown Closure)	5190	Exposed Flats
1750	Managed Wetland, in Maintained Lawn Green Space	4220	Coniferous Forest (>50% Crown Closure)	5200	Natural Lakes
5300	Artificial Lakes	6141	Phragmites Dominate Coastal Wetlands	6250	Mixed Wooded Wetlands
5400	Bays, Estuaries, and Other Tidal Waters	6200	Interior Wetlands	6251	Mixed Forested Wetlands (Deciduous Dominate)
5410	Tidal Rivers, Inland Bays, and Other Tidal Waters	6210	Deciduous Wooded Wetlands	6252	Mixed Forested Wetlands (Coniferous Dominate)
5411	Open Tidal Bays	6220	Coniferous Wooded Wetlands	6290	Un-vegetated Flats
5420	Dredged Lagoon	6221	Atlantic White Cedar Wetlands	6500	Severe Burned Wetlands
5430	Atlantic Ocean	6230	Brush Dominate and Bog Wetlands	7100	Beaches
6100	Coastal Wetlands	6231	Deciduous Scrub/Shrub Wetlands	7200	Bare Exposed Rock
6110	Saline Marshes	6232	Coniferous Scrub/Shrub Wetlands	7300	Extractive Mining
6111	Saline Marshes (Low marsh vegetation)	6233	Mixed Scrub/Shrub Wetlands (Deciduous Dominate)	7400	Altered Lands
6112	Saline Marshes (High marsh vegetation)	6234	Mixed Scrub/Shrub Wetlands (Coniferous Dominate)	7430	Disturbed Wetlands (Modified)
6120	Freshwater Tidal Marshes	6240	Herbaceous Wetlands	7500	Transitional Areas (Sites Under Construction)
6130	Vegetated Dune Communities	6241	Phragmites Dominate Interior Wetlands	7600	Undifferentiated Barren Lands

2.3 LAND USE DATASET COMPARISON TO AERIAL IMAGERY

In New Jersey, the NJLU data agreed best with the aerial imagery, which was dated 2006 (available from the Environmental Systems Research Institute's ArcGIS Online World Imagery), but because this dataset does not cover New York, a separate investigation was conducted comparing the GAP and NLCD only. Two sites in New Jersey and two sites in New York were investigated for agreement between land cover datasets and aerial imagery. Because the *surface directional effective roughness length* parameter varies most between types of development, RAMPP emphasized agreement and quality in developed areas.

Site 1 (Figure 1) was Sandy Hook, NJ, where many different types of land cover exist in a small area. The beach is backed by residential and commercial development, with some marsh and forested areas bordering the inland waterways. The NJLU dataset accurately represents the boundaries between land cover classes. Figure 1(b) shows these precise transitions between classes throughout the image, and reveals that the polygons accurately reflect the type of land cover shown in the underlying aerial image. The circled areas in Figure 1 are good for comparing the accuracy of data versus land use in the underlying aerial image. Figure 1(c) shows the coverage of the NLCD raster, which contains classification errors and also has a lower resolution than the NJLU dataset. Although the areas of light blue on the peninsula (at the center of the left hand side of Figure 1(c) are classified as Emergent Herbaceous Wetlands, the aerial images reveal that most of these areas are dominated by residential development. The GAP data in Figure 1(d) look similar in accuracy to the NLCD in Figure 1(c). Both have the same resolution, but the GAP data appear inferior at some boundaries, such as between beaches and developed areas.

All three datasets that cover New Jersey contain multiple classifications for developed land, which is important because the *surface directional effective roughness length* parameter should change according to the height and density of buildings. Developed land classifications are given unique Manning's *n* values according to the varying density of buildings visible in aerial photographs. Having many sub-categories of vegetation classes (such as the multiple classes of deciduous forest in the GAP data as listed in Table 2) is not as important, because the distinction in aerial photography is less pronounced, and all major classes are grouped under one Manning's *n* value for the *Manning's n at sea floor* parameter.

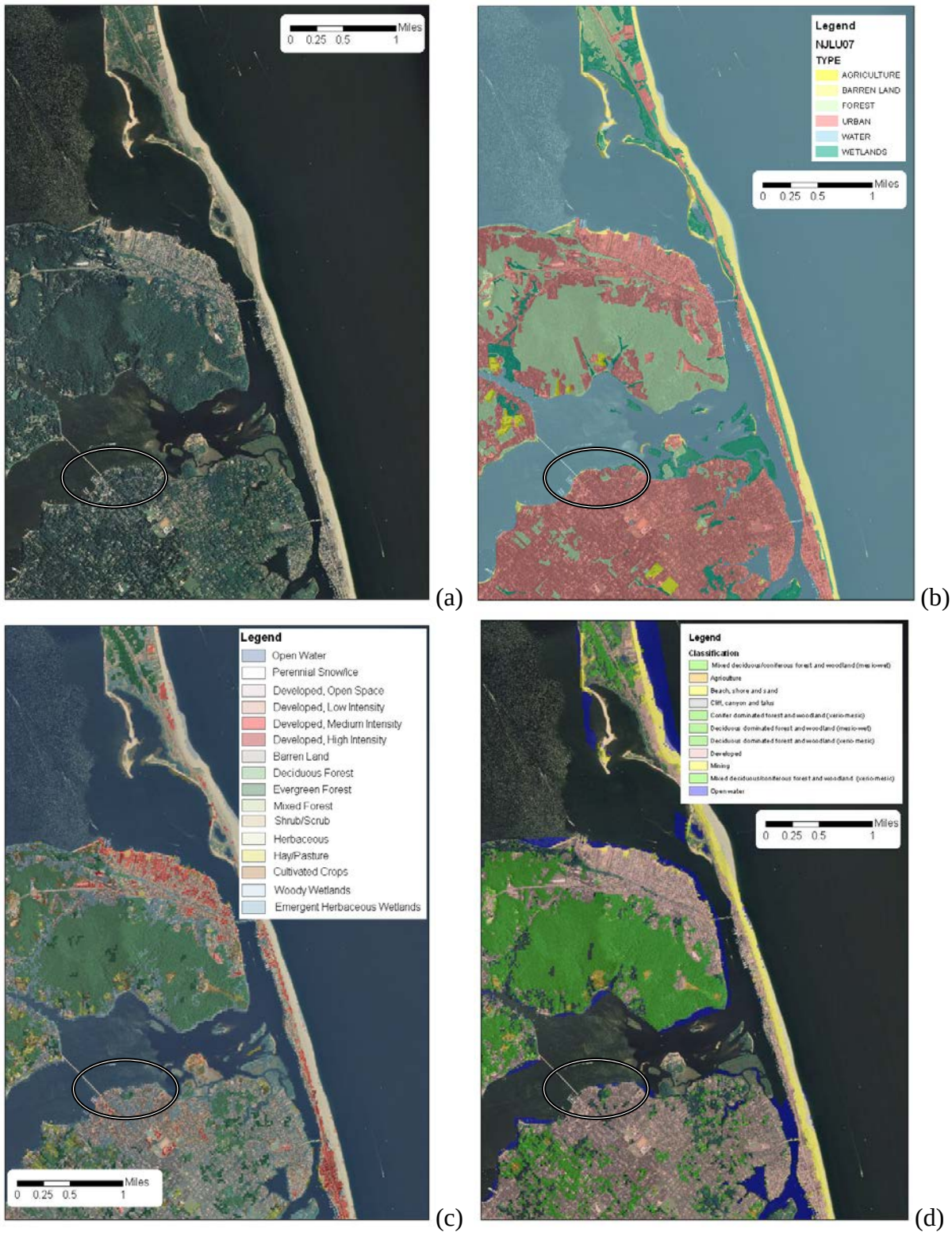

Figure 1. (a) Sandy Hook, NJ, aerial image; (b) NJLU dataset; (c) NLCD dataset; and (d) GAP dataset.

Site 2 (Figure 2) is on the southeastern shore of Cape May, NJ, which has a mix of development types ranging from high-density commercial to rural. This site allows comparison of the development classes between the datasets.

The NJLU data have seven different developed land classes ranging from Commercial/Services and High Density to Transportation and Other Urban Lands. Figure 2(b) shows that the polygons of the NJLU dataset allow the outline of specific regions of development to be characterized independently and accurately, regardless of their proximity to other features. The NLCD sporadically misrepresents the marsh and open fields in the center of Figure 2(c) as Low Intensity Development. Further, the boundaries between the four levels of development are lost to a checkerboard pattern near the coast. Because the land use traits are essentially sub-sampled onto the ADCIRC mesh nodes, the user must remove the anomalies associated with the checkerboard pattern to ensure the sub-sampled data accurately represent the land use. The GAP data also misrepresent some marsh and open fields as developed lands, but have more accurate boundaries than the NLCD. The checkerboard pattern shown in Figure 2(d) also appears in the GAP data, again raising concerns of sub-sampling anomalies.

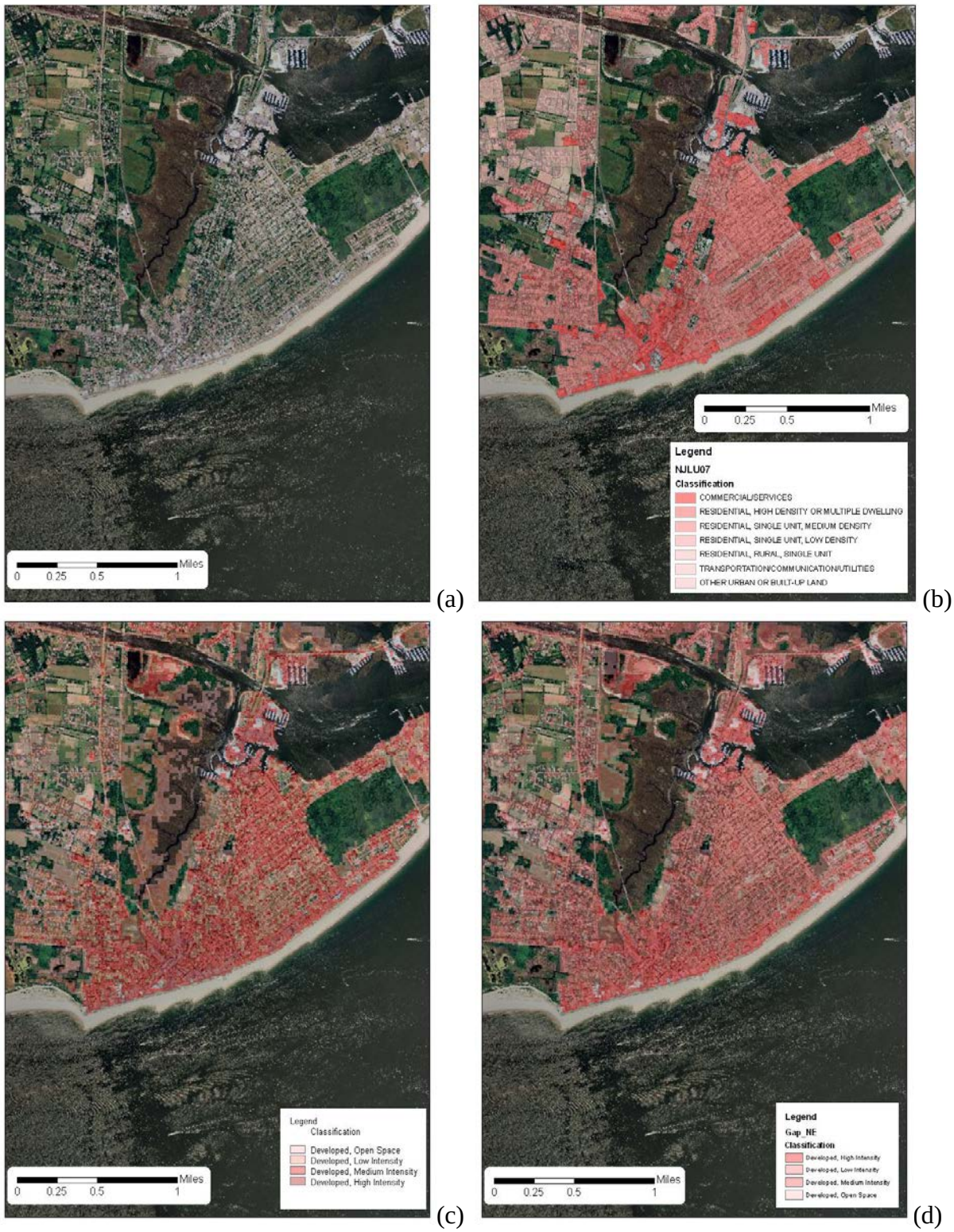

Figure 2. (a) Cape May, NJ, aerial image, (b) NJLU dataset, (c) NLCD dataset, and (d) GAP dataset.

Site 3 (Figure 3) is a section of New York City, NY, where the land cover is almost wholly urban development. Isolated areas of marsh and forest appear, which are captured in varying degrees by the GAP and NLCD datasets. Only two datasets are available to compare at Site 3, as the NJLU dataset covers only New Jersey.

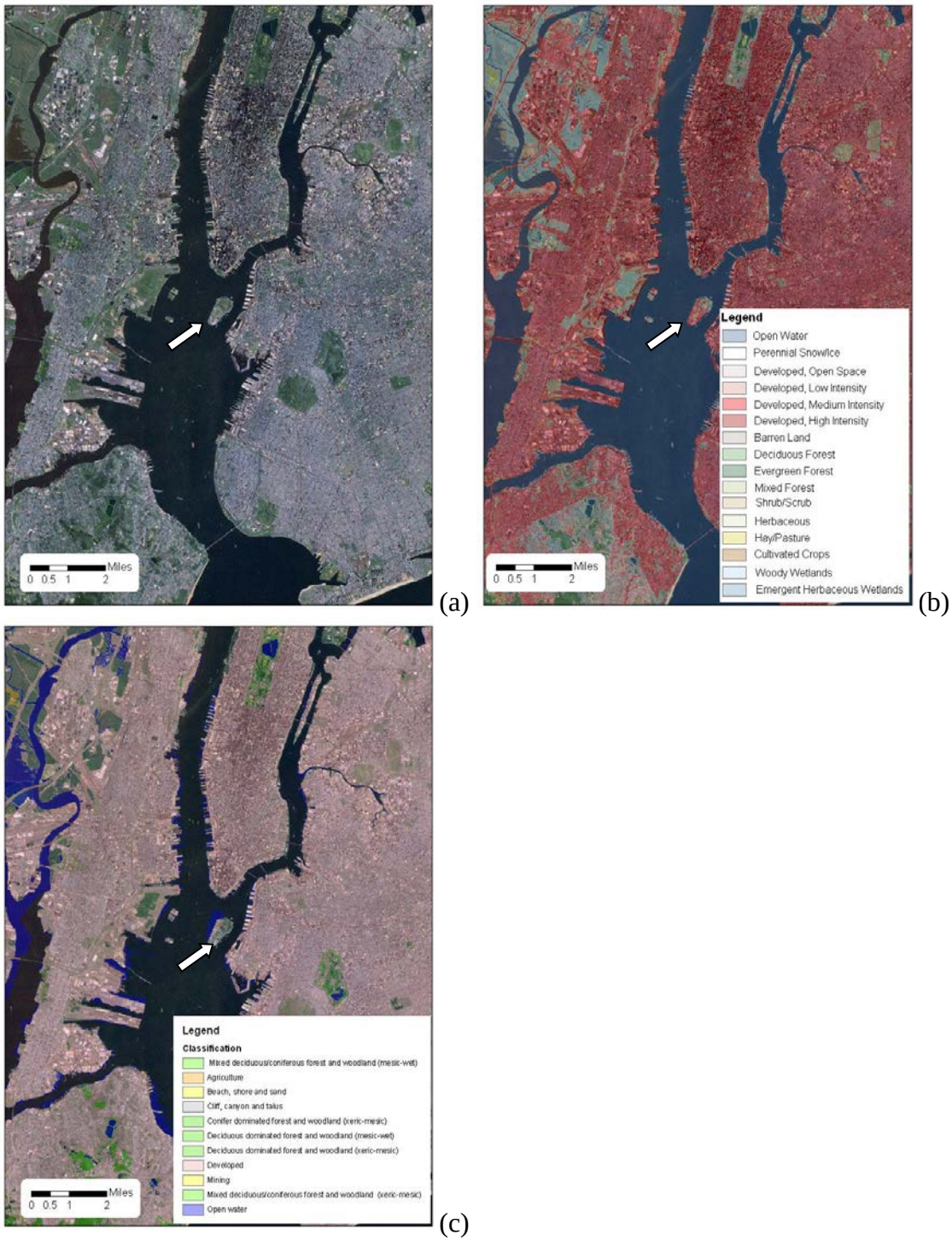

Figure 3. (a) New York City, NY, aerial image, (b) NLCD dataset, and (c) GAP dataset.

Figure 3(b) shows the consistent urban land cover represented in the NLCD dataset. Though some of the docks and river boundaries are not resolved, most of the other features are represented accurately. Because most docks are not solid obstructions to flooding, slight inaccuracies in resolving them are not critical. The boundaries in the GAP data are not as accurate as the NLCD at Site 3. A white arrow identifies a small island in Figure 3. On this island, the GAP data show only one small section of development, but the entire island should be classified as developed. Other than the differences at the boundaries and a few transportation features, the NLCD and GAP data are identical throughout the urban areas of Site 3.

Because the NLCD and GAP data are similar in areas dominated by urban development, Site 4 (Figure 4) was chosen to evaluate the respective abilities of the datasets to resolve other land cover features. The site is along the Hudson River in a typical suburban area with a mix of open fields, development, and forest.

The NLCD incorrectly classifies large areas of suburban development and forest as open space at Site 4. Some of these inaccuracies can be seen as the light blue areas of Figure 4(b). Where the aerials show forest or mixed development and forest, one suggested area of comparison is circled. The GAP data better resolve the smaller wooded areas at Site 4 that are misrepresented in the NLCD, as shown in Figure 4(c).

Figure 4. (a) Hudson River, NY aerial image, (b) NLCD dataset, and (c) GAP dataset.

2.4 FINAL LAND USE DATASET

Based on the above analysis of the existing land use data sources, the NJLU dataset was selected for use where it exists (in New Jersey). In New York State, where NJLU data are not available, the GAP data appear to be in the best agreement with aerial imagery. The two available datasets in New York are very similar in urban areas; however, the GAP data more accurately represent suburban and rural land cover types. Therefore, the GAP data in New York has been merged with the NJLU data in New Jersey to create a final land use dataset.

SECTION THREE MANNING'S N AT SEA FLOOR

The *Manning's n at sea floor* parameter is converted to an equivalent quadratic friction coefficient before the bottom stress is calculated. The bottom stress is incorporated into the ADCIRC model as a resistance to flow in the depth averaged momentum equations (Luettich et al., 1992). The Manning's n value is determined from land cover data. The program "mannings_n_finder_v10.f" on the ADCIRC website (http://adcirc.org/home/related-software/adcirc-utility-programs/) was modified and used to create the *Manning's n at sea floor* parameter. The resulting nodal attribute values can be seen in Figure 5. The original program maps land use categories from the NLCD, but the Region II Storm Surge Study team examined other land use datasets and selected the NJLU and GAP data for New Jersey and New York, respectively. A detailed comparison between the available land use datasets in the region and the *Manning's n at sea floor* values, are further described in Appendix A.

(a) 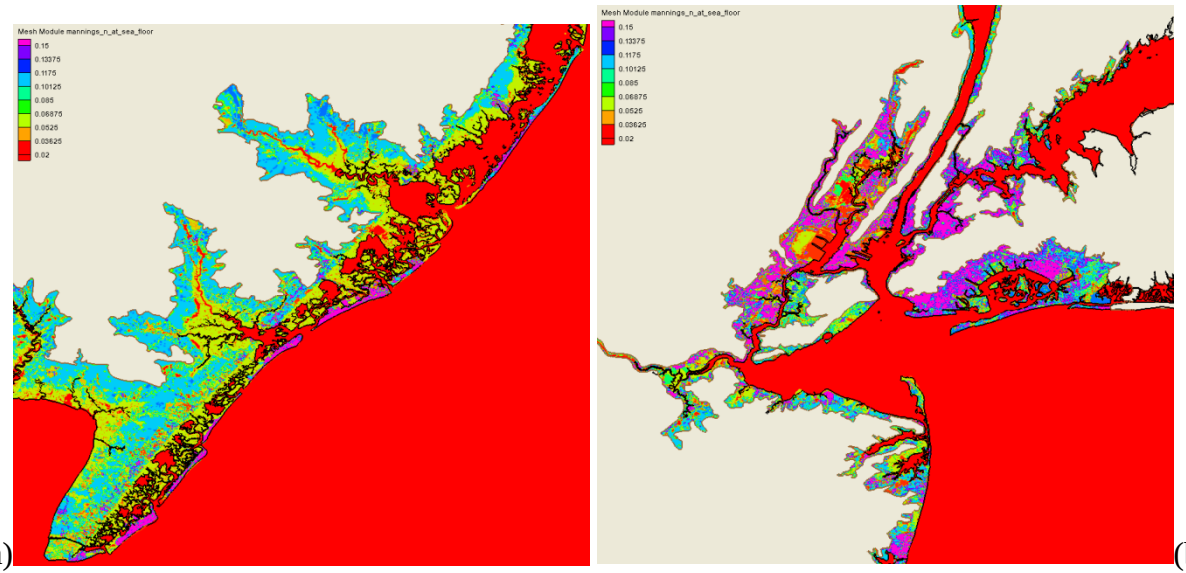

(b)

Figure 5. Nodal attribute Manning's n at sea floor in model mesh at (a) southern New Jersey, and (b) northern New Jersey and New York.

SECTION FOUR SURFACE DIRECTIONAL EFFECTIVE ROUGHNESS LENGTH

The *surface directional effective roughness length* parameter represents the wind flow in 12 directions. The roughness of the ground cover impedes wind flow coming from these 12 compass directions, starting at the location of the ADCIRC grid node and extending 3.2 kilometers radially in each of the 12 directions. Roughness length relates to the height of the ground cover. This is translated into the amount of "shielding" from the wind and water column that is incorporated into the model. On this scale, open water is smooth and would not impede wind flow, but a skyscraper would be considered very rough. The translation between the height of the ground cover and the shielding are based on work done with the Federal Emergency Management Agency's (FEMA's) Hazus model (Axe, 2003). Hazus is a nationally applicable standardized methodology that contains models for estimating potential losses from earthquakes, floods, and hurricanes.

The program "surface_roughness_calc_v13.f" on the ADCIRC website (http://adcirc.org/home/related-software/adcirc-utility-programs/) was used to create the *surface directional effective roughness length* parameter. This program was designed to map various NLCD types to surface roughness lengths. This program was modified for use in the Region II Storm Surge Study to use NJLU and GAP land use types. The GAP and NJLU land use datasets each have a large number of classifications, many of which cannot be differentiated from the point of view of surface roughness on winds. These codes were simplified by mapping a range NJLU and GAP land use codes to their NLCD equivalents, and applying the NLCD *surface directional effective roughness length* parameter values (from the original "surface_roughtness_calc_v13.f" program). The mapping was done manually by review of the class names and spot checks on aerial imagery. These codes are provided in Table 4.

Table 4. Land use code mapping for the *surface directional effective roughness length* parameter.

NLCD Code	GAP Code	NLCD Code	Coefficient
1400-1411, 1419	2100-2199	11	0.001
1440-1499, 1700-1799, 5000-5999, 1420, 7500	1201	21	0.1
1800-1899, 1130, 1140, 2300	1202	22	0.3
1120, 1150, 1600	1203	23	0.4
1200-1300, 1110, 1500	1204	24	0.55
7200, 7300, 7400, 7430,7600	1301, 3105, 8103, 8501	31	0.04
7100	3100 3104, 3106 3199, 7503	32	0.9
4100-4199, 4500	4100-4199,7507, 8401	41	0.65
4200-4299	4539-4540, 4551, 8401	42	0.72
4300-4399	8200-8299, 4211	43	0.71
4410-4411		51	0.1

NLCD Code	GAP Code	NLCD Code	Coefficient
4420, 4430, 4440	4300-4399, 5807, 8107	52	0.12
2400		71	0.04
2100	1402, 8108	81	0.06
2200		82	0.06
6210-6229, 6250-6259	1403, 9235, 3240, 9308 9803, 9818, 9820, 9843	91	0.55
6230-6234; 2140, 2150		92	0.12
6130	9914	94	0.12
6290	8102, 9501	95	0.11
6240-6249		96	0.11
6100-6120, 6141, 6500	9200-9234, 9236-9239 9241-9299, 8406, 9101, 9109, 9819	97	0.11

Figure 6 shows a sample of the *surface directional effective roughness length* parameter values in southern New Jersey. This figure shows the roughness or shielding of the wind in 12 directions. Red and orange areas have less roughness or shielding, since the wind is blowing over open water in these areas. Greens and blues show increasing shielding of the wind as it blows over rougher terrain, including buildings and forests. The direction of the wind is shown in the lower right corner of each figure.

After completion of the final production runs, an error was found in the utility program to create the surface directional effective roughness length parameter (the surface_roughness_calc_v14.f program). An analysis of this error is described in Appendix B. The error was shown to have little impact on the final results, therefore the original model runs were retained and the information described above regarding this parameter is valid.

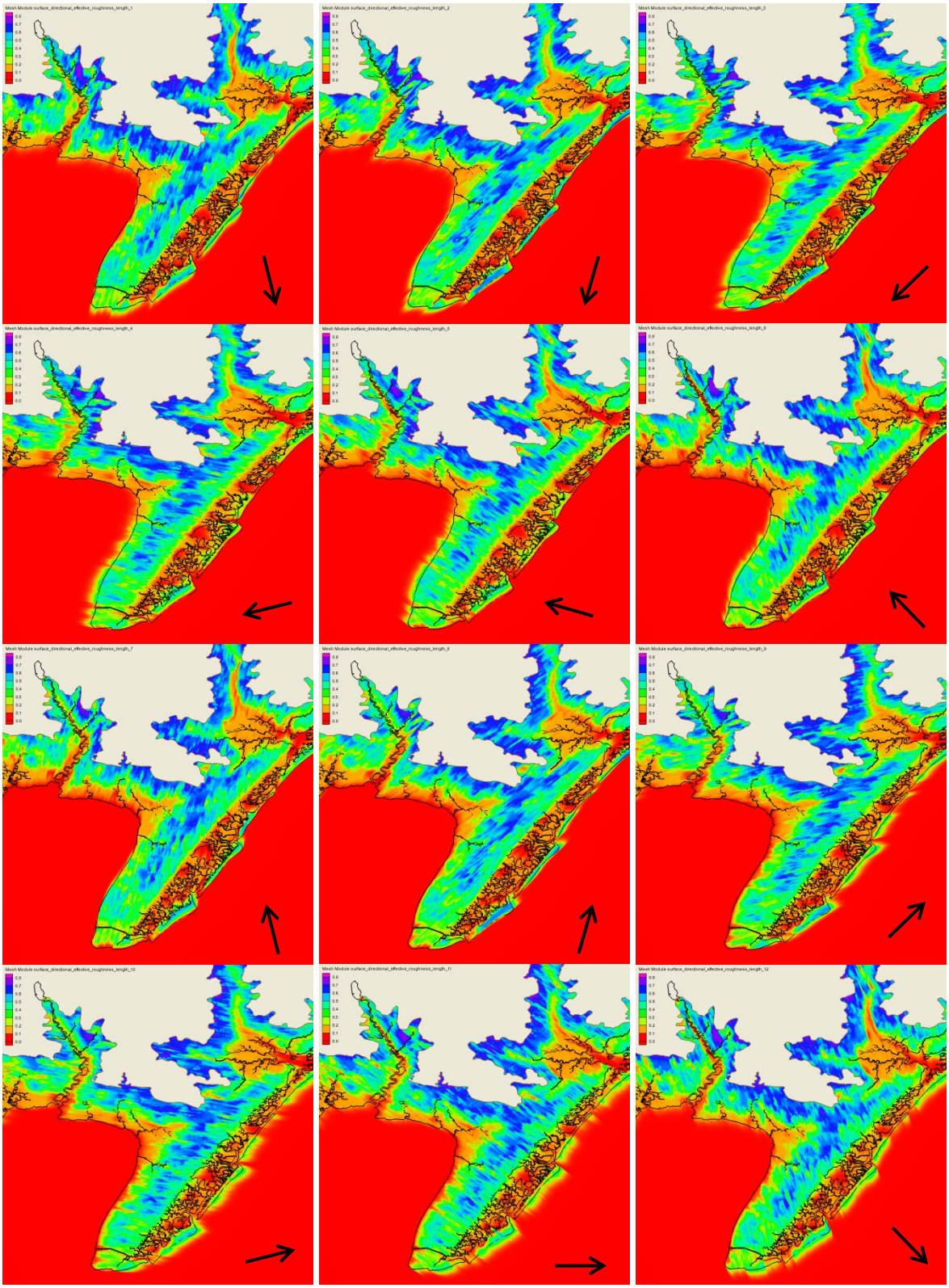

Figure 6. Nodal attribute surface directional effective roughness length in model mesh.

SECTION FIVE SURFACE CANOPY COEFFICIENT

The *surface canopy coefficient* parameter allows the user to turn off wind stress in heavily forested areas because the canopy shields the water from the effect of the wind. Reid and Whitaker (1976) have shown that in heavily forested canopies, the momentum transfer from the wind field to the water column is minimal. In ADCIRC, this theory is translated into a binary parameter such that a value of 0 indicates no wind stress because of a canopy; otherwise the value is set to 1 and the wind stress is unchanged.

The *surface canopy coefficient* has been determined in previous studies using only the NLCD classes, but for this study, the NJLU and GAP data sets were used. The program "surface_canopy_v4.f" available on the ADCIRC website (http://adcirc.org/home/related-software/adcirc-utility-programs/) was modified to handle NJLU and GAP land use codes. The NJLU dataset have an advantage over the NLCD for determining the *surface canopy coefficient* because the quaternary level of classification in forested areas characterizes the canopy closure percentage, as seen in Figure 7. For instance, a polygon classified as forested could have either 10 to 50 percent canopy closure, or >50 percent canopy closure. If the tree canopy is closed by less than 50 percent, wind stress could still be imparted on the water surface, so the *surface canopy coefficient* was set to 1. In contrast, wind stress is less likely to be imparted on the water surface with a canopy closure greater than 50 percent, so the *surface canopy coefficient* was set to 0. Areas of forest that yield a *surface canopy coefficient* of 1 allow wind stress to be applied to the water surface, although at a rate limited by the *surface directional effective roughness length* (Westerink et al., 2008). For those areas where the NJLU data are available, that dataset has been used to determine the *surface canopy coefficient*; the GAP dataset has been used elsewhere. The land use codes selected to set the *surface canopy coefficient* to 0 have been listed in Table 5 and 6.

A sample of the surface canopy coefficient values in the mesh is shown in Figure 8.

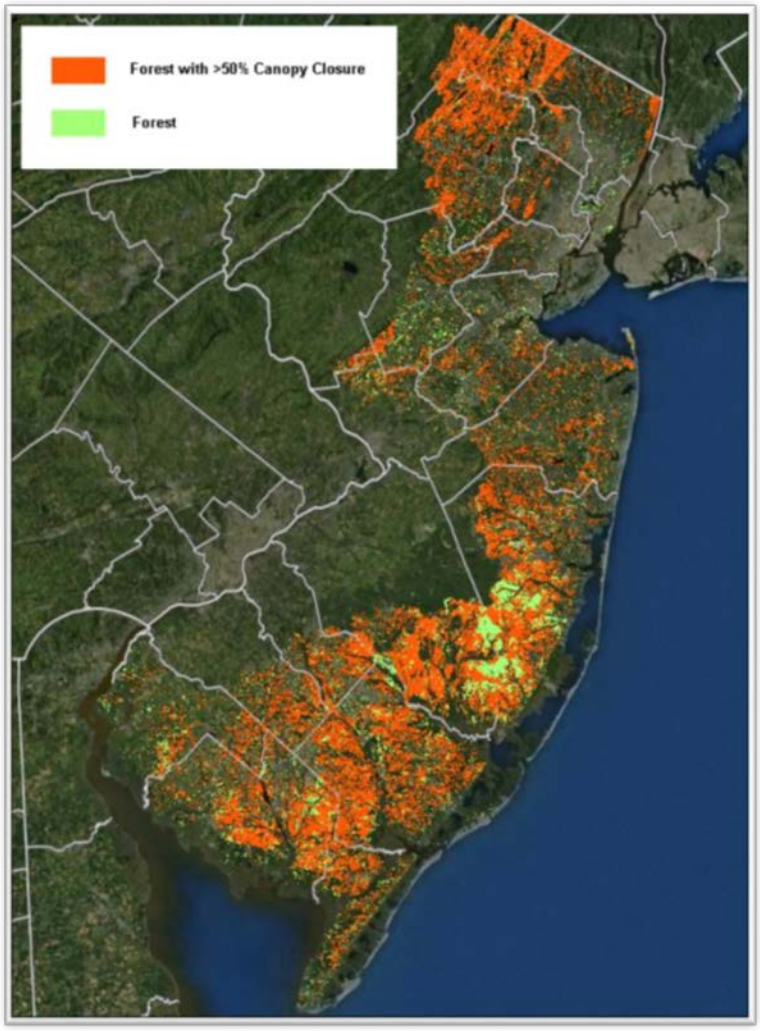

Figure 7. Map of New Jersey showing the spatial difference between all forested areas and forested areas with more than 50 percent canopy closure in the NJLU dataset.

Table 5. NJLU classes selected to set *surface canopy coefficient* to 0.

NJLU Code	Land Cover Description
4120	Deciduous forest (>50% crown closure)
4220	Coniferous forest (>50% crown closure)
4312	Mixed forest (>50% coniferous >50% crown closure)
4322	Mixed forest (>50% deciduous >50% crown closure)

Table 6. GAP classes selected to set *surface canopy coefficient* to 0.

GAP Code	Land Cover Description
4104	Northeastern Interior Dry Oak Forest - Hardwood Modifier
4113	Laurentian-Acadian Northern Hardwoods Forest
4114	Northeastern Interior Dry - Mesic Oak Forest
4133	Atlantic Coastal Plain Dry and Dry-Mesic Oak Forest
4211	Atlantic Coastal Plain Northern Maritime Forest
4313	Northern Atlantic Coastal Plain Dry Hardwood Forest
4323	Laurentian-Acadian Northern Pine-(Oak) Forest
4327	Laurentian-Acadian Pine-Hemlock-Hardwood Forest
4330	Central Appalachian Oak and Pine Forest
4331	Appalachian Hemlock-Hardwood Forest
4335	Central Appalachian Pine-Oak Rocky Woodland
4539	Northeastern Interior Pine Barrens
4551	Acadian-Appalachian Montane Spruce-Fir Forest
8202	Evergreen Plantation or Managed Pine
8203	Managed Tree Plantation
8504	Ruderal Wetland and Forest
9240	Northern Atlantic Coastal Plain Basin Swamp and Wet
9308	Laurentian-Acadian Alkaline Conifer-Hardwood Swamp
9843	Atlantic Coastal Plain Small Blackwater River Floodplain

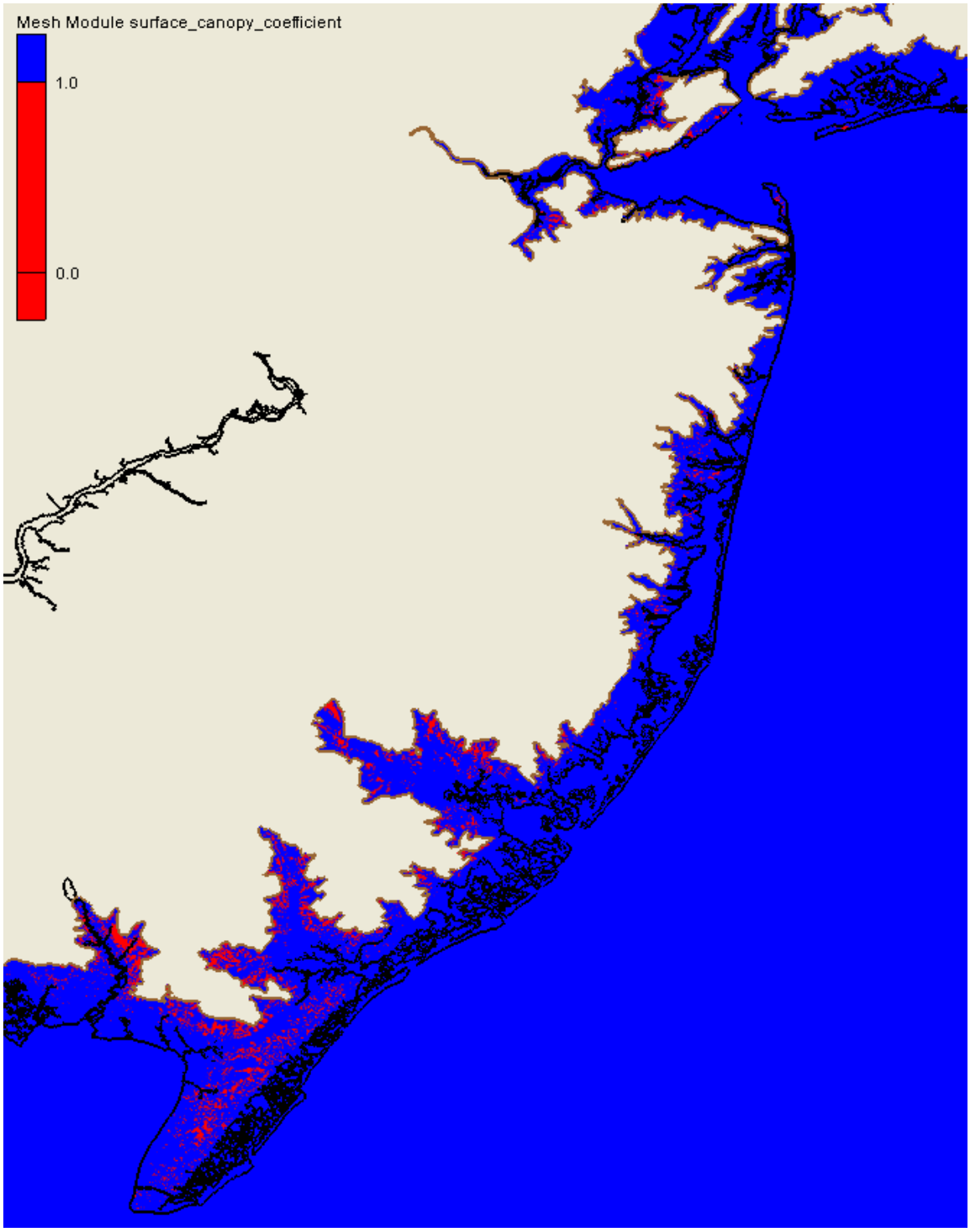

Figure 8. Nodal attribute surface canopy coefficient in model mesh.

SECTION SIX WAVE REFRACTION IN UNSWAN

The *wave refraction in SWAN* parameter is used to set where refraction is or is not calculated in the mesh by UnSWAN. Because wave refraction is a highly localized process that occurs over short distances in shallow waters, high mesh resolution is necessary to accurately model the process. The coupled UnSWAN and ADCIRC models use the same mesh, which covers a large region spanning the northwest Atlantic Ocean, including many distant islands and seamounts between Florida and South America, most of which are represented at low resolution. These areas do not have an appreciable effect on waves or storm surge in the study area, and are mainly needed for accuracy in determining the tides. However, as a result of the low resolution of these shallow areas, wave refraction can cause spurious spikes in wave heights that are detrimental to the model. To avoid this, wave refraction is only calculated in a selected region around the study area. This area is bounded by a rectangle from 35.701°, -77.028° to 42.816°, -71.069°, as shown in Figure 9. The nodal parameter *wave refraction in SWAN* is set to enable wave refraction in the model wherever the nodal attribute is set to "1," and disable it wherever it is set to "0." The program "refrac_select.f90" was built in-house to create the *wave refraction in SWAN* parameter.

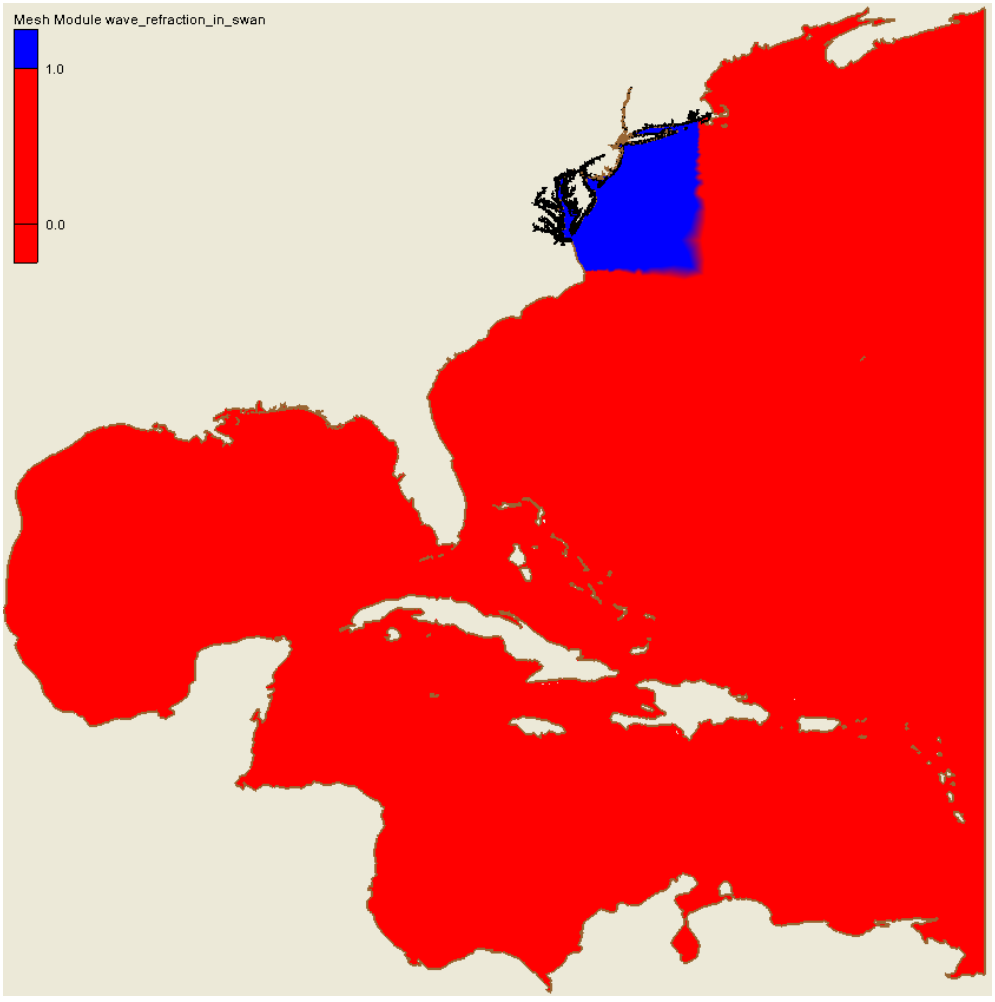

Figure 9. Nodal attribute wave refraction in UnSWAN in model mesh.

SECTION SEVEN PRIMITIVE WEIGHTING IN CONTINUITY EQUATION

The *primitive weighting in continuity equation* parameter sets the τ_0 parameter, controlling the relative contribution of the primitive and wave portions of the Generalized Wave-Continuity Equation, which is a reformulation of the shallow water equations used by the ADCIRC model. This balance is such that for τ_0, a value of 0 is the pure wave equation and a value greater than 1 behaves like a pure primitive continuity equation. Typical values for the *primitive weighting in continuity equation* parameter are in the range of 0.005 to 0.1.

The program "tau0_gen.f" on the ADCIRC website (http://adcirc.org/home/related-software/adcirc-utility-programs/) was used to create the *primitive weighting in continuity equation* parameter. The parameter was set by finding the average distance between a node and its neighbors (as determined by the element connectivity between nodes). If the average distance between neighboring nodes was less than 1,750 meters, then the τ_0 parameter was set to 0.03. Otherwise, the value was set to 0.005 for depths greater than 10 meters and 0.02 for depths less than or equal to 10 meters. These values were also used for ongoing FEMA storm surge studies in North Carolina and South Carolina. The values assigned in the Region II study area can be seen in Figure 10.

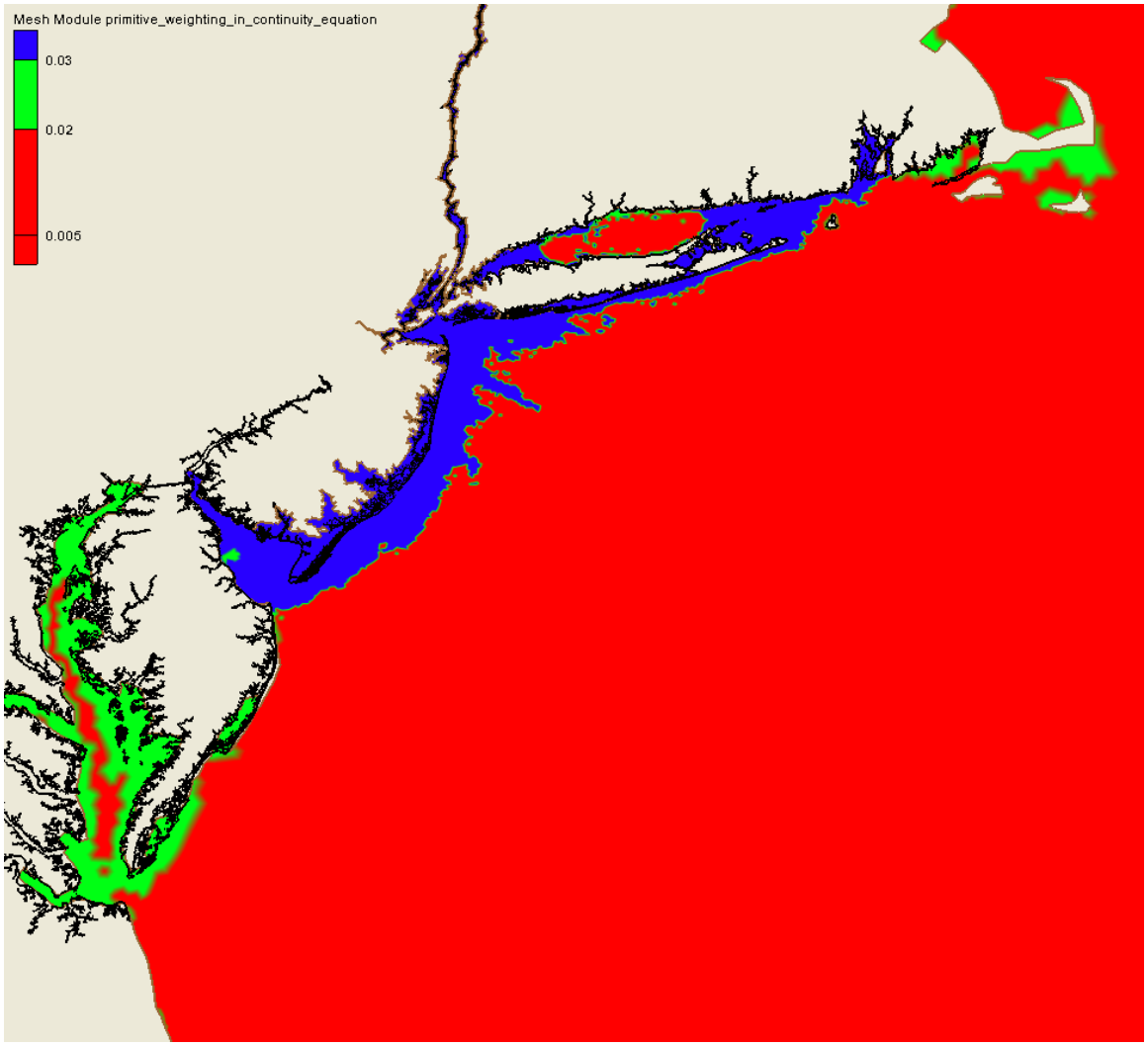

Figure 10. Nodal attribute primitive weighting in continuity equation in model mesh.

SECTION EIGHT REFERENCES

Axe, L.M., Hurricane Surface Wind Model for Risk Management, Florida State University, 2003, http://diginole.lib.fsu.edu/cgi/viewcontent.cgi?article=1038&context=etd

Chow, V.T., Open-channel hydraulics. New York, McGraw-Hill Book Co., 1959, 680 pp.

Luettich, R.A., Jr., J.J. Westerink, and N.W. Scheffner, ADCIRC: an advanced three-dimensional circulation model for shelves coastal and estuaries, report 1: theory and methodology of ADCIRC-2DDI and ADCIRC03DL, Dredging Research Program Technical Report DRP-92-6, U.S. Army Corps of Engineers Waterways Experiment Station, Vicksburg, MS, 1992, 137 pp.

Reid, R.O. and R.E. Whitaker, Wind-Driven Flow of Water Influenced by a Canopy, Journal of the Waterways, Harbors and Coastal Engineering Division, Proceedings of the American Society of Civil Engineering, Volume 102, Number WW1, 1976, pp 61–77.

Westerink, J.J., R.A. Luettich, J.C. Feyen, J.H. Atkinson, C. Dawson, H.J. Roberts, M.D. Powell, J.P. Dunion, E.J. Kubatko, and H. Pourtaheri, A Basin- to Channel-Scale Unstructured Grid Hurricane Storm Surge Model Applied to Southern Louisiana. Monthly Weather Review, 136:3, 2008, pp. 833–864.

APPENDIX A

Manning's *n* Value Selection

INTRODUCTION

There has not been extensive research on how to associate Manning's *n* values with individual land cover classifications. Although Chow's classic text (Chow 1959) is over 50 years old, it is still considered accurate guidance for Manning's *n* values; however, his research (and others') provides appropriate values for natural and manmade channels, and not overbank areas. Some work has been done to determine acceptable values for tall vegetation and structures that need to be represented in overland surge models. The recent (and ongoing) FEMA storm surge studies for North Carolina, South Carolina, Mississippi, Louisiana, Texas, and northwest Florida provide a basis for determining Manning's *n* values in New York and New Jersey for similar land cover classes. As an extension of the research into the appropriate land use data to use for this study, the Manning's *n* values for the NJLU, National Land Cover Dataset, and Gap Analysis Program data were determined.

Manning's *n* values for the GAP data are based on previous studies and values that are based on Chow's work (Chow 1959), but some new land use categories (particularly with the NJLU dataset) were found. If a new land class appeared in a dataset that had not been used in previous studies, a Manning's *n* value was assigned by comparing aerial photographs of similar land classes and qualitatively interpolating a reasonable value for the new land class. Considering how other datasets classified the same areas was also helpful. New land classes offer the opportunity to refine the assignment of Manning's *n* values to specific types of land cover rather than to make broad assignments.

Although categories may have similar names between datasets, the way they classify land cover varies. For instance, all three datasets contain a class entitled "low intensity development." Both the NJLU's and GAP's versions of this class were assigned n=0.05. But the NLCD's version was assigned n=0.1, because the NLCD "low intensity developed" regions and "medium intensity developed" regions cover very similar developed areas that are the same as GAP and NJLU "medium intensity development" classes, according to the aerial photograph comparison. The GAP and NJLU "medium intensity development" classes were assigned n=0.1. In this way, some of the values assigned in the NLCD data were adjusted, so this study could be consistent with the more detailed GAP and NJLU data.

The NJLU and GAP datasets contain numerous redundant classes. For the following tables of proposed Manning's *n* values, the redundant classes were grouped together to facilitate easier comparison among datasets. Table A-1 presents the proposed Manning's *n* values according to land cover provided by the NJLU dataset. Typical ranges of values for similar land cover taken from Chow (1959) are also listed in Table A-1.

Table A-2 contains the Manning's *n* values according to the NLCD for given land cover classes found in the region. The advantage of the NLCD is that its coverage is national, facilitating comparison between the proposed values and those used in previous studies. The Manning's *n* defined for the NLCD data has also been standardized for use in HAZUS analysis. Also provided is a range of values from Chow (1959) for reasonable Manning's *n* value comparison, as well as links to a website with photographs that correspond to most of the classification types as compiled by NOAA's Coastal Services Center.

Table A-3 presents the Manning's *n* values associated with the GAP data for the Northeast GAP dataset. Also listed in Table A-3 for comparison is a range of appropriate Manning's *n* values from Chow (1959).

Table A-1. NJLU proposed Manning's *n* values based on land cover

NJLU Code	Land Cover Description	NJ/NY Manning's *n*	Chow (1959) Manning's *n* Range
1110	Residential, High Density or Multiple Dwelling	0.15	
1120	Residential, Single Unit Medium Density	0.1	
1130	Residential, Single Unit Low Density	0.05	
1140	Residential, Rural Single Unit	0.05	
1150	Mixed Residential	0.1	
1200s	Commercial and Services	0.15	
1300	Industrial	0.15	
1400s*	Transportation/Communication/Utilities	0.025	
1419	Bridge Over Water (Open Water)	0.02	
1440	Airport Facilities	0.05	
1500	Industrial and Commercial Complexes	0.15	
1600	Mixed Urban or Built-up Land	0.1	
1700s	Other Urban (Open Space)	0.03	
1800s	Recreational Land	0.025	
2100	Cropland and Pastureland	0.035	0.025-0.05
2140	Agricultural Wetlands (Cranberry Farms, etc.)	0.048	
2150	Former Agricultural Wetlands (Becoming Shrubby not	0.035	
2200	Orchards, Vineyards, Nurseries, Horticultural Areas, Sod	0.037	0.025-0.05
2300	Confined Feeding Operations	0.075	
2400	Other Agriculture	0.04	
4110s, 4120s	Deciduous Forest	0.1	0.08-0.2
4210s, 4220s	Coniferous Forest	0.11	0.08-0.2
4230	Plantation	0.07	
4310s, 4320s	Mixed Forest	0.1	0.08-0.2
4410s	Fields	0.035	0.025-0.05
4410s	Fields	0.035	0.025-0.05
4420, 4430, 4440	Brush/Scrubland	0.05	0.035-0.16
4500	Severe Burned Upland Vegetation	0.07	
5000s	Open Water	0.02	0.016-0.033
6100–6200, 6240s	Marshes/Wetlands	0.05	0.05-0.08
6130	Vegetated Dune Community	0.048	
6210s, 6220s,	Wooded Wetlands	0.1	0.075-0.15
6230s	Brush Dominated and Bog Wetlands	0.05	0.05-0.08
6290	Un-vegetated Flats	0.025	
6500	Severe Burned Wetlands	0.045	
7100	Beaches	0.025	
7200	Bare Exposed Rock, Rockslides, Mining, etc.	0.08	
7300	Extractive Mining	0.08	
7400	Altered Lands	0.08	
7430	Disturbed Wetlands (Modified)	0.045	
7500	Transitional Areas (Sites Under Construction)	0.03	
7600	Undifferentiated Barren Lands	0.025	0.025-0.05

*Manning's n value used for all codes in this range with the exception of the sub-classifications listed below

Table A-2. Proposed Manning's *n* values according to the NLCD

NLCD Code	Land Cover	NJ/NY Manning's n	Chow (1959) Manning's n Range	Example Photographs
11	Open Water	0.02	0.016-0.033	http://www.csc.noaa.gov/crs/lca/class_groups/water.html
12	Perennial Snow/Ice	0.01		
21	Developed, Open Space	0.05		http://www.csc.noaa.gov/crs/lca/class_groups/osd.html
22	Developed, Low Intensity	0.1		http://www.csc.noaa.gov/crs/lca/class_groups/lid.html
23	Developed, Medium Intensity	0.1		http://www.csc.noaa.gov/crs/lca/class_groups/mid.html
24	Developed, High Intensity	0.15		http://www.csc.noaa.gov/crs/lca/class_groups/hid.html
31	Barren Land	0.04	0.025-0.05	http://www.csc.noaa.gov/crs/lca/class_groups/bl.html
41	Deciduous Forest	0.1	0.08-0.2	http://www.csc.noaa.gov/crs/lca/class_groups/df.html
42	Evergreen Forest	0.11	0.08-0.2	http://www.csc.noaa.gov/crs/lca/class_groups/ef.html
43	Mixed Forest	0.1	0.08-0.2	http://www.csc.noaa.gov/crs/lca/class_groups/mf.html
52	Shrub/Scrub	0.05	0.035-0.16	http://www.csc.noaa.gov/crs/lca/class_groups/ss.html
71	Herbaceous	0.035	0.025-0.05	http://www.csc.noaa.gov/crs/lca/class_groups/gl.html
81	Hay/Pasture	0.035	0.025-0.05	http://www.csc.noaa.gov/crs/lca/class_groups/ph.html
82	Cultivated Crops	0.037	0.025-0.05	http://www.csc.noaa.gov/crs/lca/class_groups/cl.html
90	Woody Wetlands	0.1	0.075-0.15	
95	Emergent Herbaceous Wetlands	0.05	0.05-0.08	

Table A-3. Proposed Manning's *n* values based on land cover represented by the Northeast GAP raster

GAP Classification Code	Land Cover	NJ/NY Manning's *n*	Chow (1959) Manning's *n* Range
1201	Developed, Open Space	0.025	
1202	Developed, Low Intensity	0.05	
1203	Developed, Medium Intensity	0.1	
1204	Developed, High Intensity	0.15	
1301	Quarries, Mines, Gravel Pits, Oil Wells	0.09	
1402	Cultivated Cropland	0.035	0.025-0.05
1403	Pasture/Hay	0.035	0.025-0.05
2100s	Open Water	0.02	0.016-0.033
3100s	Beach, shore and sand	0.04	
4100's	Deciduous dominated forest	0.1	0.08-0.2
4211, 4300s	Mixed deciduous/coniferous forest	0.1	0.08-0.2
4539	Conifer Dominated Forest	0.11	0.08-0.2

GAP Classification Code	Land Cover	NJ/NY Manning's *n*	Chow (1959) Manning's *n* Range
4540	North Atlantic Coastal Plain Pitch Pine Barrens	0.09	
4551	Acadian-Appalachian Montane Spruce-Fir Forest	0.1	
5807	Northern Atlantic Coastal Plain Heathland and Grassland	0.05	
7503	Atlantic Coastal Plain Southern Dune and Maritime Grassland	0.035	0.025-0.05
7507	Northern Atlantic Coastal Plain Dune and Swale	0.035	
8102	Disturbed/Successional-Shrub Regeneration	0.055	0.035-0.08
8103	Disturbed/Successional-Grass/Forb Regeneration	0.04	
8107, 08	Harvested forest-Shrub Regeneration	0.05	0.035-0.16
8200s	Evergreen Plantation or Managed Pine	0.11	0.08-0.2
8401	Introduced Vegetation (Forest)	0.1	0.08-0.2
8406	Introduced Vegetation (Wetland)	0.045	
8501	Other Disturbed or Modified Land	0.08	
8504	Other Disturbed or Modified (Wooded Wetland)	0.1	
9101	Acadian Salt Marsh and Estuary Systems	0.025	
9109	Salt, Brackish and Estuary Wetland	0.05	0.05-0.08
9200s*	Freshwater Herbaceous Marsh, Swamp, or Baygall	0.05	0.05-0.08
9224	Freshwater Herbaceous Marsh, Swamp, or Baygall (Shrub)	0.05	0.05-0.08
9235	Freshwater Herbaceous Marsh, Swamp, or Baygall (Wooded)	0.1	0.075-0.15
9308	Laurentian-Acadian Alkaline Conifer-Hardwood Swamp	0.1	
9501	Boreal Acidic Peatland Systems	0.025	
9800's, 9900's	Mixed Deciduous/Coniferous Riparian Forest	0.1	

* Manning's n value used for all codes in this range with the exception of the sub-classifications listed below

The results of interpolation of the data onto ADCIRC mesh nodes are shown in the figures below. The sites are the same location as those in the main report. Site 1, Sandy Hook, NJ, contains a variety of land use types at various spatial scales. The NJLU data accurately represents this variety as shown in Figure A-1 below. Note that the nodes do not cover the entire land area in the figure; the ADCIRC mesh was typically terminated at the +25-foot land elevation contour.

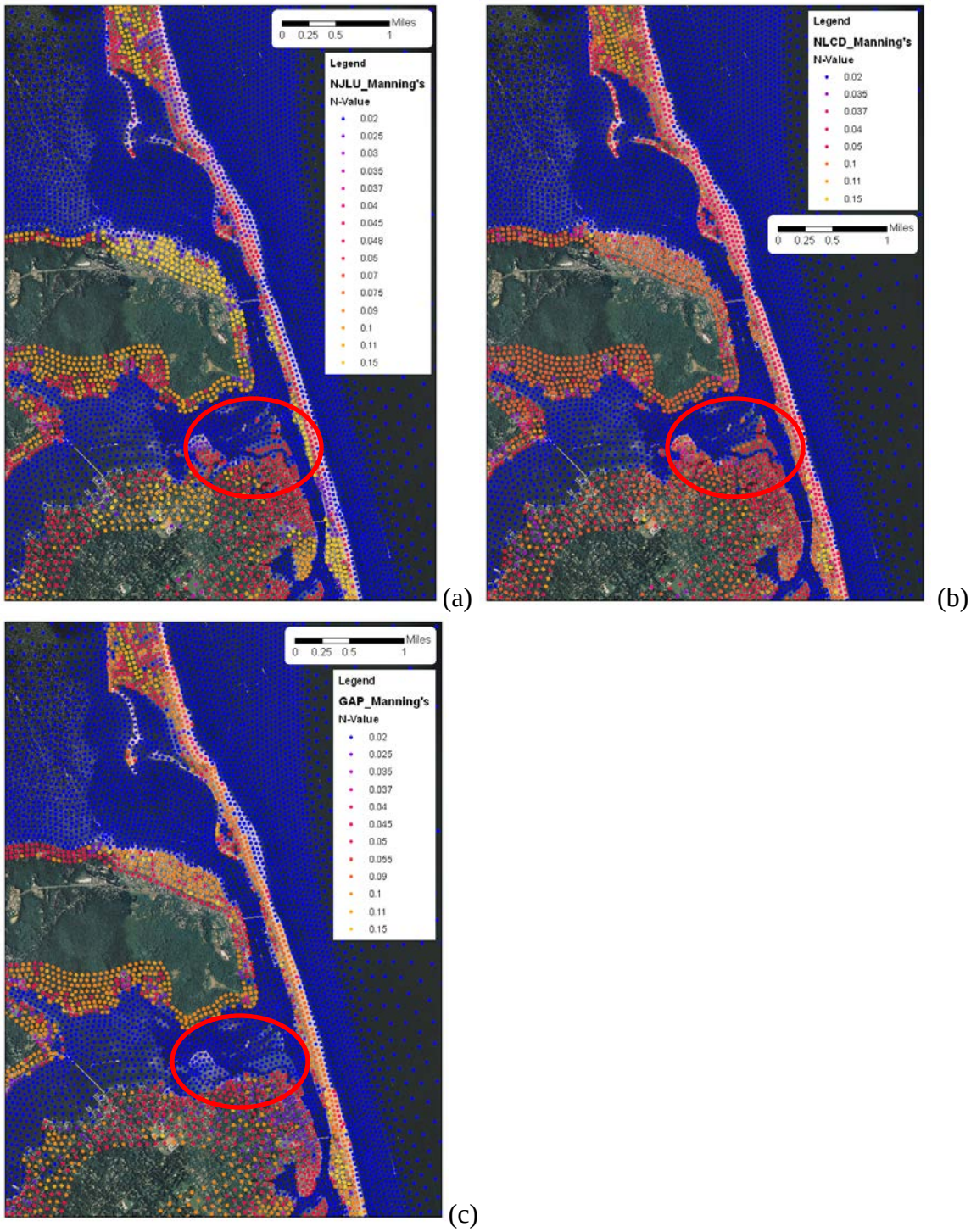

Figure A-1. Manning's *n* according to (a) NJLU, (b) NLCD, and (c) GAP datasets at Site 1, Sandy Hook, NJ.

The most noticeable difference between Figure A-1 (a) and the NLCD-derived values in Figure A-1 (b) is the number of distinct Manning's *n* values. Since the NLCD contains fewer land use classifications, it is restricted to fewer unique Manning's *n* values. Although the GAP dataset has

many more land use categories than the NLCD dataset, it has fewer categories than the NJLU dataset. The GAP data misrepresent some land cover at the shoreline, as seen in the circled center of Figure A-1 (c) where a large portion of land is assigned n=0.02, which is the value assigned to open water.

Site 2, Cape May, NJ, is a predominantly residential area, with interspersed fields, forests, and streams. The higher number of NJLU classifications results in a better approximation of the ground roughness across varied land cover types. Figure A-2 (a) shows Manning's *n* values according to NJLU data. Note to the left of the figure that the Manning's *n* values are distinct over each variation in land cover, from open field to developed area to forest.

Figure A-2 (b) shows Manning's *n* values derived from the NLCD data, and Figure A-2 (c) shows them for the GAP data for the same region. There are not as many Manning's *n* values represented as a result of the coarseness of these data sources compared to the NJLU data.

Site 3, New York City is not covered by the NJLU data since it is in New York. Figure A-3 (a) shows Manning's *n* values from the NLCD data, and Figure A-3 (b) shows them from the GAP data at Site 3 on the ADCIRC mesh nodes. The NLCD better resolves the shoreline boundaries than the GAP data, and so Manning's *n* values at the ADCIRC mesh nodes also better represent these boundaries. While both the NLCD and GAP data contain four urban classes, the GAP data differentiate between more types of vegetated lands.

Site 4, Hudson River in Westchester County, NY, has a broader range of land use types, and so offers a better vantage point for evaluating the difference between NLCD and GAP data. East of the river, the right-hand-side in Figure A-4 (a), the NLCD was assigned an excessively low value of 0.05 where it classified the land as Developed, Open Space. This *n* value can be seen over both forested areas and developed areas, where it does not represent a proper roughness for these land cover types. The GAP data more accurately represent the forested and developed land, so the places where the Manning's *n* value are too low in Figure A-4 (a) have more accurate Manning's *n* values in Figure A-4 (b).

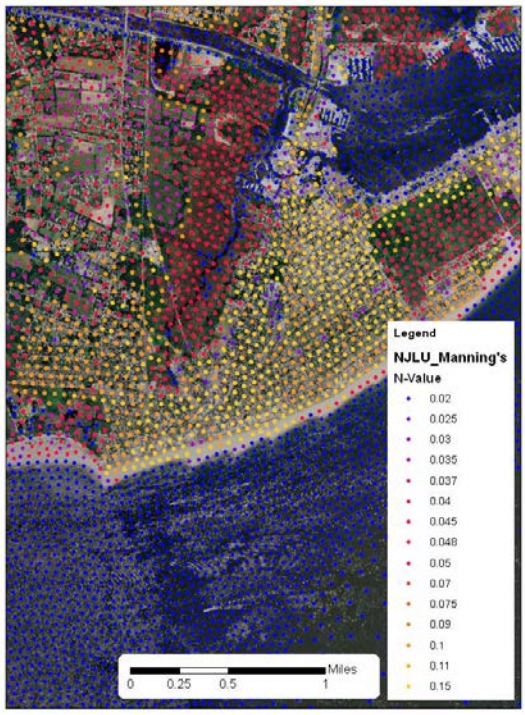

(a)

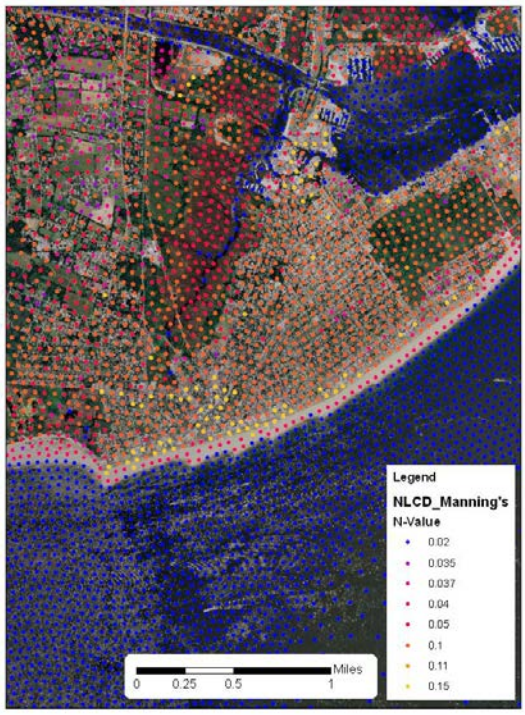

(b)

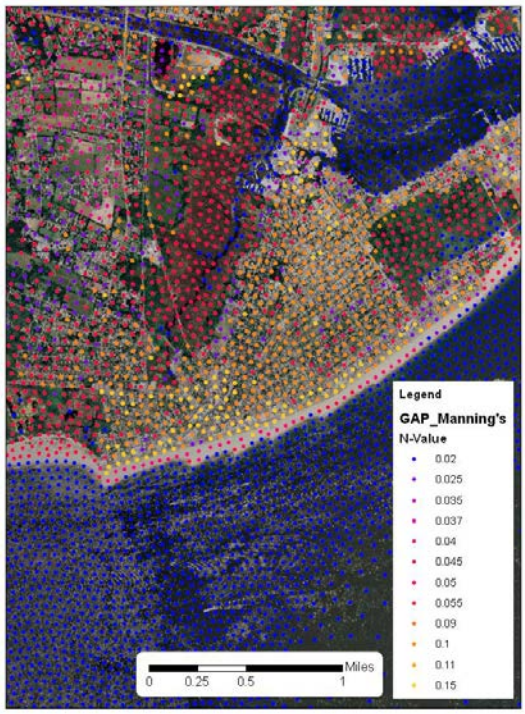

(c)

Figure A-2. Manning's *n* according to (a) NJLU, (b) NLCD, and (c) GAP datasets at Site 2, Cape May, NJ.

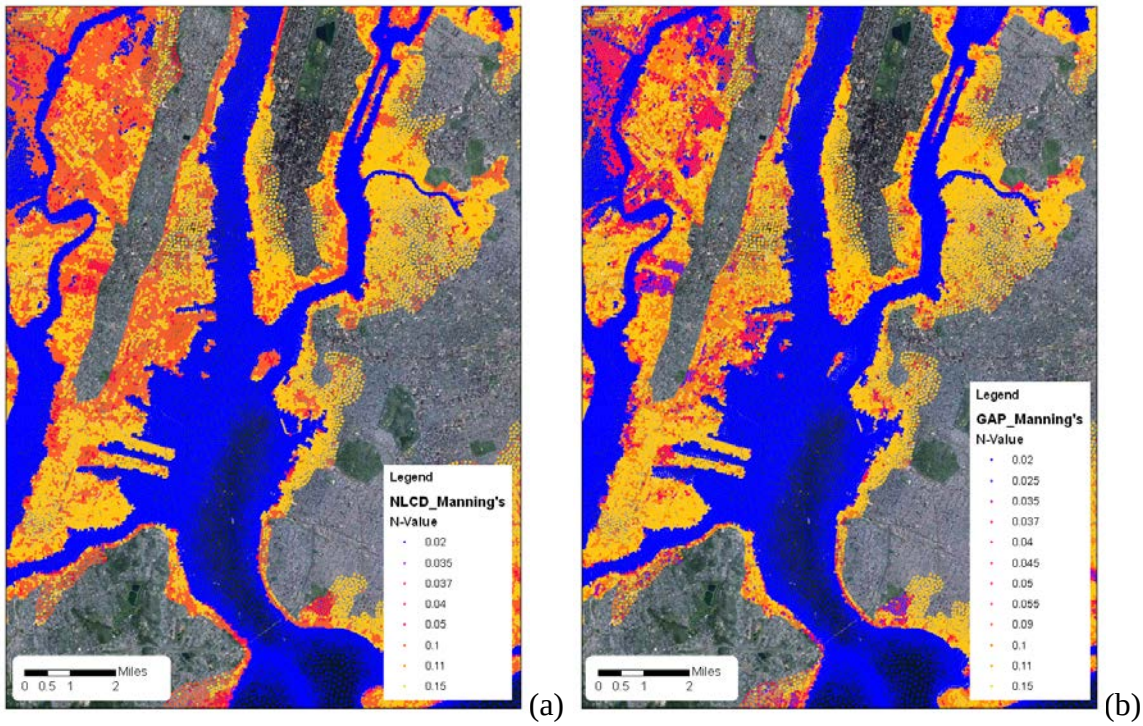

Figure A-3. Manning's *n* according to (a) NLCD and (b) GAP datasets at Site 3, New York City, NY.

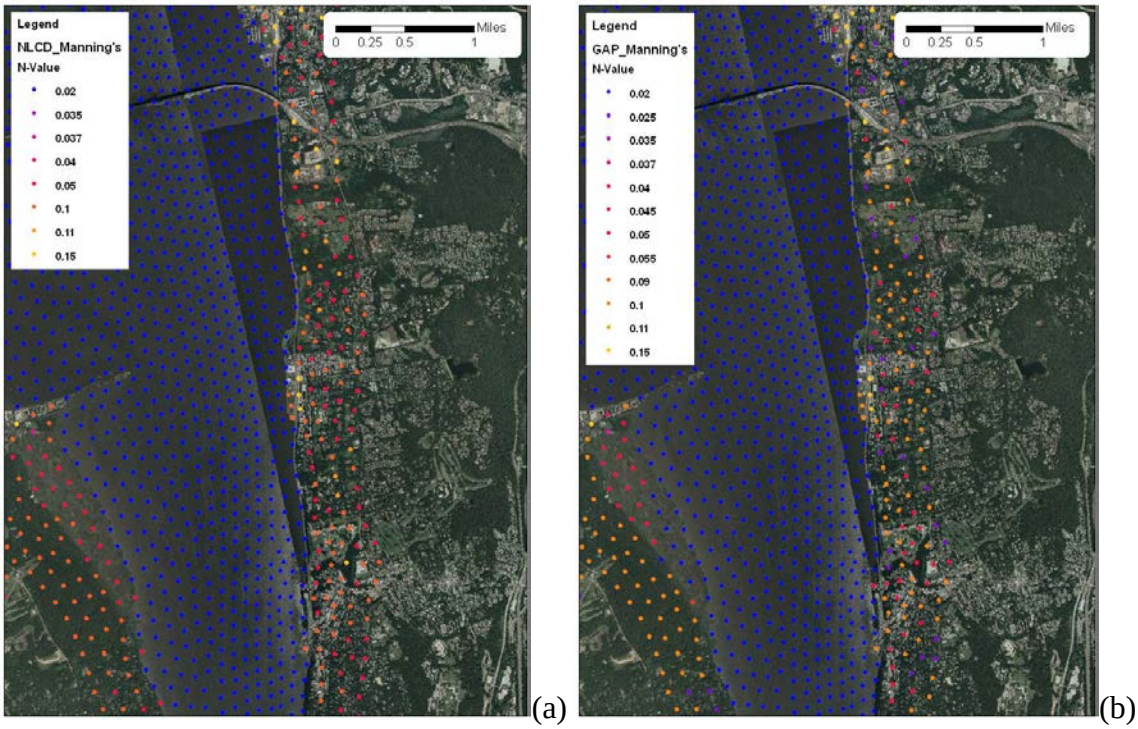

Figure A-4. Manning's *n* according to (a) NLCD and (b) GAP datasets at Site 4, Westchester County, NY.

APPENDIX B

Impacts of an Error in the Directional Land Roughness Length Program on Storm Surge Calculations Using the ADCIRC Model

INTRODUCTION

During the study, it came to the attention of the FEMA storm surge modeling teams that an error existed in an open source preprocessing code used by several modeling groups to prepare one of the input files used in storm surge simulation with the ADCIRC model. The code in question, surface_roughness_calc_v14.f (and earlier versions), is one of several Fortran codes used for pre-processing input files for ADCIRC that are provided freely to the ADCIRC community by the model developers at the University of North Carolina at Chapel Hill. The error resulted in an incorrect ordering of the directional land roughness lengths contained in an ADCIRC input file (fort.13). The directional land roughness lengths are used to reduce the wind speed at nearshore and onshore locations in the ADCIRC domain depending on the type of land cover, such as buildings, marsh, or trees, present in the upwind direction. Twelve directional land roughness lengths (spaced every 30 degrees around the compass dial) are provided for each ADCIRC node to account for the presence of different land cover types in different upwind directions. While the preprocessing code computed the land roughness lengths correctly, they were written in the wrong order to the fort.13 and thus interpreted by ADCIRC as corresponding to an incorrect upwind direction.

The erroneous preprocessing code was used to create the directional land roughness lengths for four FEMA coastal storm surge studies, namely the FEMA Region II study for New Jersey and New York City; the FEMA Region III study for Delaware, Maryland, Virginia, and Pennsylvania; the North Carolina study being performed by the State of North Carolina as a Cooperating Technical Partner (CTP); and the South Carolina study being performed by the State of South Carolina as a CTP. Each of these four storm surge studies had previously completed their Joint Probability- Optimum Sampling production storm simulations and was in the final stage of review of the calculated return periods when this issue was identified. Other FEMA studies that are in progress or were completed recently are not impacted by this issue because they used a different preprocessing code that did not contain the error, or they are using a recently corrected code.

This document details the issue, explains the actions taken to evaluate the magnitude of the impacts, and provides a basis for the conclusions and resolution of the issue.

ISSUE

The ADCIRC model incorporates the directional land roughness lengths at each grid node assuming that values start in the due east direction and proceed in a counterclockwise direction for each of the 12 directional bins. The incorrect data in the fort.13 file created by the pre-processing code commenced at due north and listed the coefficients for each of the 12 directional bins in a clockwise direction. While all internal information was accurate, the direction specified in creating the input file was incorrect. In areas where the wind reduction lengths were the same or similar in all or a group of wind directions, it is not expected that inaccuracies were introduced. In areas where the wind reduction lengths change quickly and by a large value from one compass direction to the next, greater impacts on individual storm results may be found. This may be most prevalent close to any land/water interface where there is a low reduction to

winds blowing in the onshore direction and larger reductions to winds blowing in the offshore direction. Hence, depending on the track of an individual storm and the associated direction of the winds, there will be varying impacts from one storm to the next.

The sensitivity of changes to the directional wind roughness length are expected to be small as a component of total wind drag or wind stress for each storm simulated. The directional wind roughness length is not applied directly to input wind speeds. Instead, this roughness length comprises one factor in the formulation of the total wind drag or wind stress applied to the water surface that result in storm surge.

Wind Stress: $\boldsymbol{\tau} = \rho_a C_d |\mathbf{W}_{10}| \mathbf{W}_{10}$

Wind Drag: $C_d = (0.75 + 0.067|\mathbf{W}_{10}|)x10^{-3}$

Land winds: $\mathbf{W}_{10land} = \mathbf{W}_{10marine} [\frac{Z_{omarine}}{Z_{oland}}]^{0.0706}$

$\boldsymbol{\tau}$ = Wind Stress
$\boldsymbol{\rho_a}$ = Density of Air
$\mathbf{W_{10}}$ = Wind Velocity
$\mathbf{C_d}$ = Wind Drag
$\mathbf{Z_{omarine}}$ = Directional Marine Roughness Length
$\mathbf{Z_{oland}}$ = Directional Land Roughness Length

SOLUTION

The ADCIRC model developers have corrected the problem and have provided a revised Fortran code that creates the directional wind reduction lengths and the input to the fort.13 file correctly.

STUDY EVALUATION

Upon learning of this issue, RAMPP promptly created a corrected version of the fort.13 input file that included the directional wind reduction lengths. RAMPP began sensitivity testing to assess the impacts on the Region II storm surge model results.

The Region II study team first focused on the Jamaica Bay area of New York, selecting a group of production storms that most influence the 1-percent- annual-chance levels and simulating them with the corrected file. Initially, 12 storms were selected for the sensitivity tests, and a return period analysis was conducted with the updated storm surge values. To gain further confidence in the results and a better sense of how the return period analysis would be impacted based on the number of storms selected for the sensitivity testing, an additional 11 storms were selected and run for the Jamaica Bay area, for a total of 23 storms. Again the return period analysis was rerun with the updated surge values for these 23 storms.

The Region II study team then looked at other locales within the study area and incorporated an additional 14 storms that most influenced the 1-percent-annual-chance surge levels. These locales included the New York/New Jersey harbor area, Barnegat Bay, and Great Egg Harbor Bay, NJ (Cape May and Atlantic Counties). This resulted in a total of 37 production storms; these were rerun and return periods were again reanalyzed to determine updated surge levels for the 1-percent-annual-chance event. These 37 storms were inclusive of both tropical and extratropical events.

RESULTS

Initial results showed that for individual storms, when comparing the updated surge levels with the original levels, differences were less than 0.1 foot for the majority of the study area. There were isolated differences of plus and minus 0.5 foot in back bay areas, and in rare locations differences reached upwards of 1.0 foot. These larger differences were observed primarily at the upstream end of tributaries. An example of these differences within the Township of Toms River, NJ, is shown in Figure B-1, panels A through C, where positive values indicate an increase using the new fort.13 input file. Panel A shows the difference in the directional wind reduction lengths for a wind blowing in an east-to-west direction, Panel B shows the effect on the maximum wind speeds for one of the production storms (NJB_0005_006) which tracked north offshore the New Jersey coast, and Panel C shows the differences in the surge for the same storm.

In looking at the comparisons in Figure B-1, Panel A shows that, with the corrected fort.13 input file, the directional wind reduction lengths are reduced along the longitudinal axis of the waterway identified as Toms River in the figure, for a westerly wind. Panel B shows that the maximum winds simulated for a particular storm are higher in this same waterway, which can be attributed to the lower wind reduction lengths shown in Panel A. Panel C shows the increase in maximum surge elevations at the head of the waterway, as one would expect, as a result of the increased maximum winds. The increase in surge elevations within Toms River ranges up to 1.0 foot.

The return period analysis was then performed with the revised storm surge levels for all 37 storms. When comparing to the original results, differences from the 1-percent-annual-chance surge elevations were less than 0.1 foot for most of the study area. The differences in the 1-percent-annual-chance surge elevations are shown spatially for different areas within the entire modeled region in Figures B-2 through B-15. Figure B-9 shows the differences in the 1-percent-annual-chance stillwater elevations (SWELs) for the Toms River area, where larger differences were observed in the individual storm comparisons. At the upstream end of the river, the difference in the 1-percent-annual-chance SWELs is 0.1 to 0.2 foot.

Table B-1 shows the range of differences and the percentage of modeled points that fall into those ranges. As shown in Table B-1, out of 585,012 points evaluated, over 99% of the points showed differences to the 1-percent-annual-chance surge elevations less than 0.1 feet.

CONCLUSIONS

Overall, the 1% annual chance SWELs for the Region II study area were shown to be generally insensitive to the adjustments made to the directional wind reduction lengths when using the corrected fort.13 ADCIRC input file. Although more significant differences were seen in individual storm comparisons (0.5 to 1.0 foot), the return period analysis resulted in differences in the 1-percent-annual-chance SWELs of less than 0.1 foot for most of the study area. Locations where differences in the 1-percent-annual-chance SWELs were greater than 0.1 foot were closely examined, and it was determined that these differences would not affect the Base Flood Elevation or the extent of the flood hazard area.

These rather small differences in the 1-percent-annual-chance SWELs are also within the expected accuracy of the predicted surge elevations, given the overall context and complexity of

the storm surge modeling effort. The results from the sensitivity testing conducted provide technical justification for moving forward with the original study results, as significant impacts were not observed.

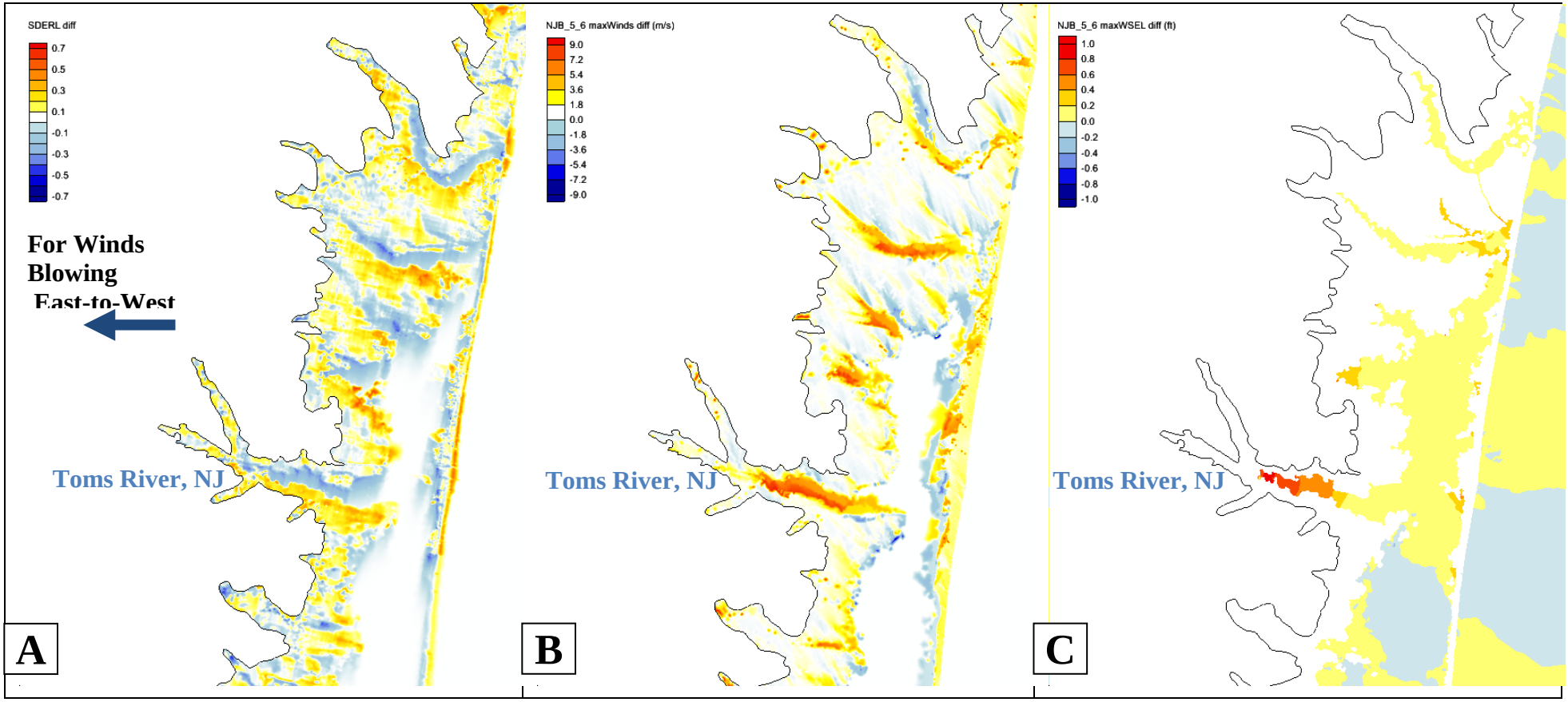

Figure B-1. For an area within Barnegat Bay, NJ, comparing the original results with those obtained using the corrected fort.13 input file, Panel A shows the difference in directional wind reduction length for a westerly wind, Panel B shows the difference in the maximum winds simulated during a production storm, and Panel C shows the difference in the maximum simulated surge levels for the same storm.

Table B-1. Summary of differences in the 1%-annual-chance SWELs when using updated results for 37 production storms

Range (feet)	Count	%
-0.7 - -0.6	6	0.00%
-0.6 - -0.5	1	0.00%
-0.5 - -0.4	7	0.00%
-0.4 - -0.3	23	0.00%
-0.3 - -0.2	29	0.00%
-0.2 - -0.1	998	0.17%
-0.1 - 0.0	489711	83.71%
0.0 - 0.1	94058	16.08%
0.1 - 0.2	90	0.02%
0.2 - 0.3	31	0.01%
0.3 - 0.4	12	0.00%
0.4 - 0.5	11	0.00%
0.5 - 0.6	4	0.00%
0.6 - 0.7	29	0.00%
0.7 - 0.8	1	0.00%
0.8 - 0.9	0	0.00%
0.9 -1.0	0	0.00%
1.0 -1.1	0	0.00%
1.1 -1.2	0	0.00%
1.2 -1.3	0	0.00%
1.3 -1.4	0	0.00%
1.4 -1.5	0	0.00%
1.5 -1.6	0	0.00%
1.6 -1.7	1	0.00%
	585012	**100%**

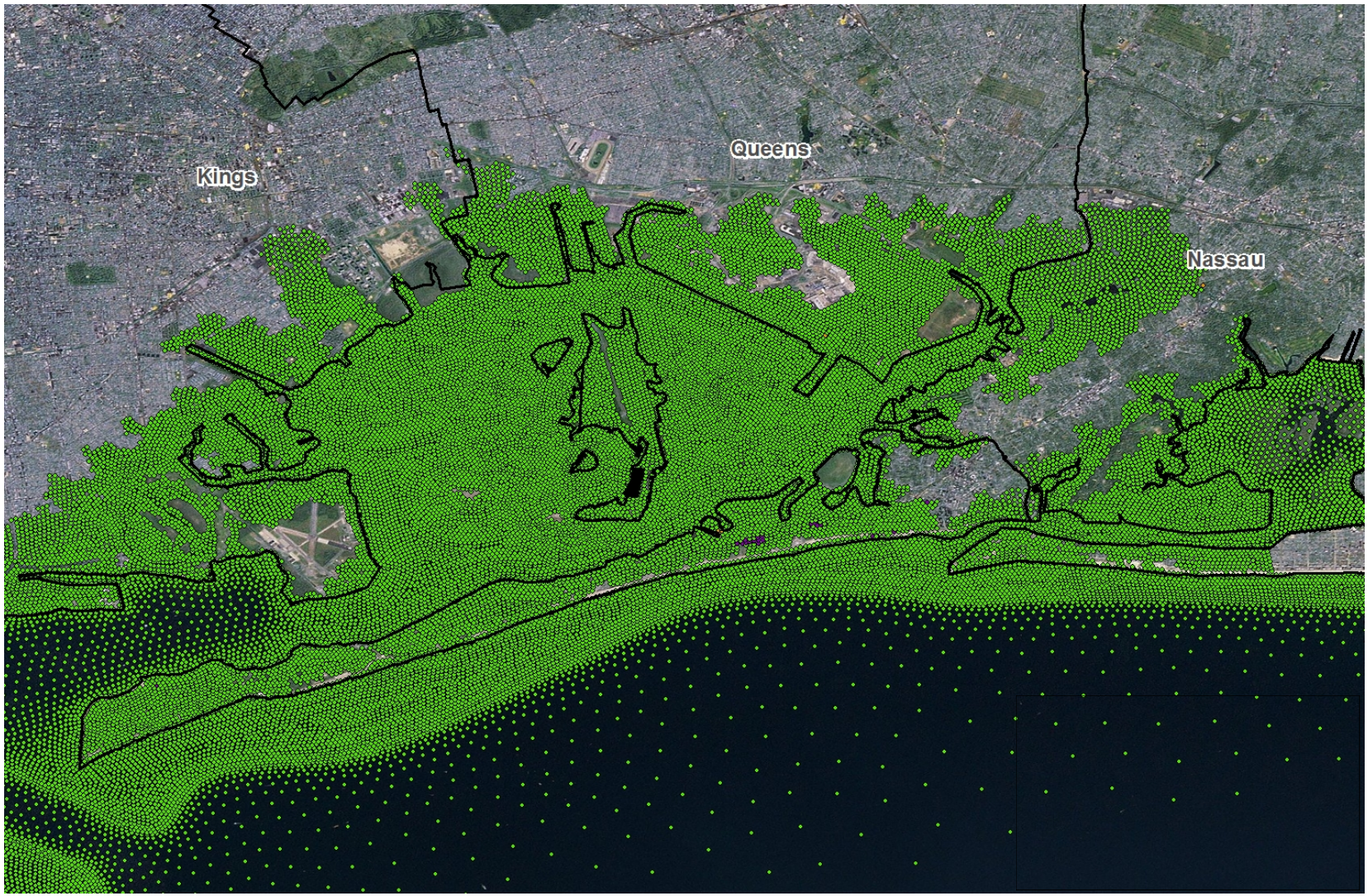

Figure B-2. Differences in 1%-annual-chance SWEL when comparing updated results from sensitivity testing (37 storms) to original results.

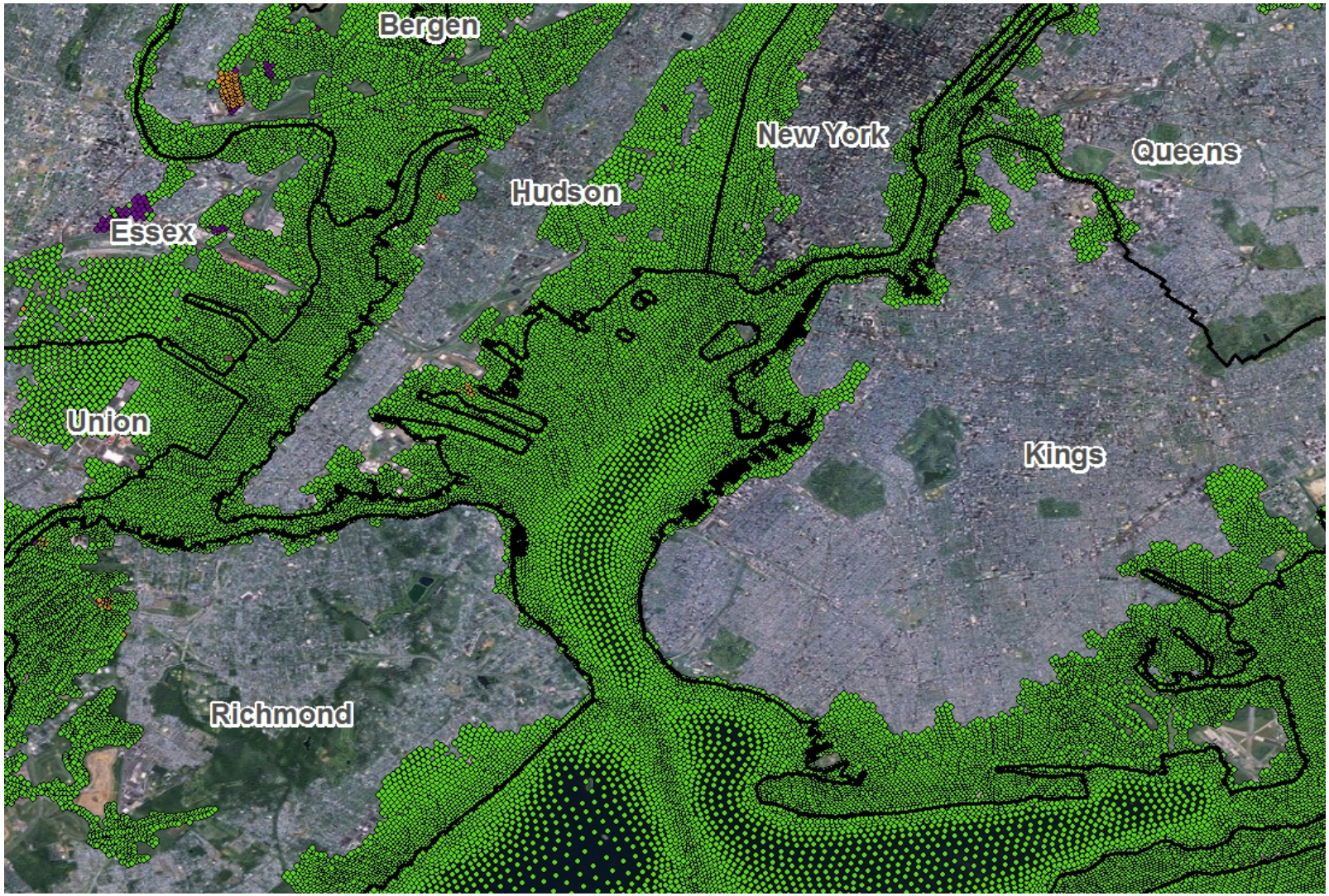

Figure B-3. Differences in 1%-annual-chance SWEL when comparing updated results from sensitivity testing (37 storms) to original results.

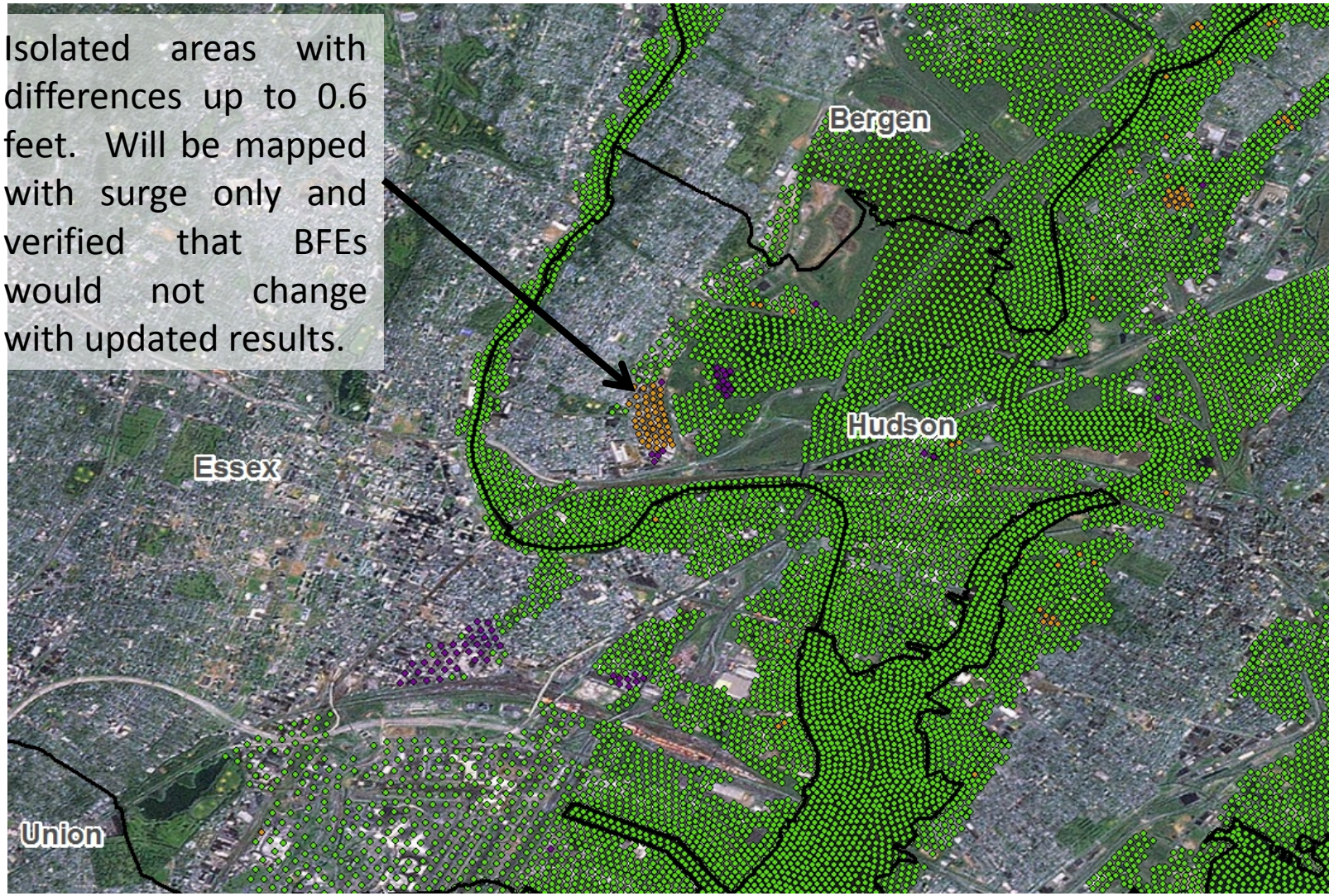

Figure B-4. Differences in 1%-annual-chance SWEL when comparing updated results from sensitivity testing (37 storms) to original results.

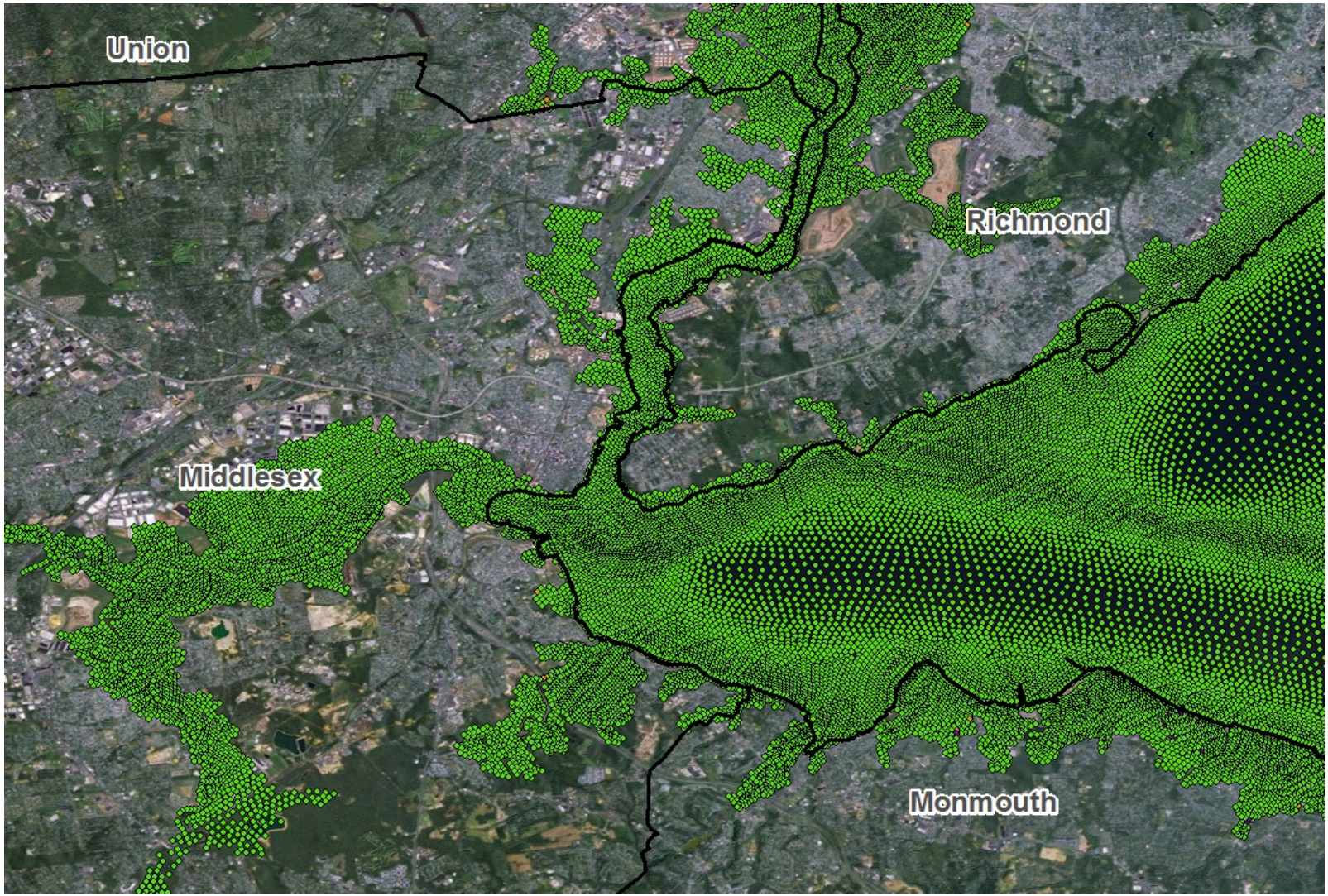

Figure B-5. Differences in 1%-annual-chance SWEL when comparing updated results from sensitivity testing (37 storms) with original results.

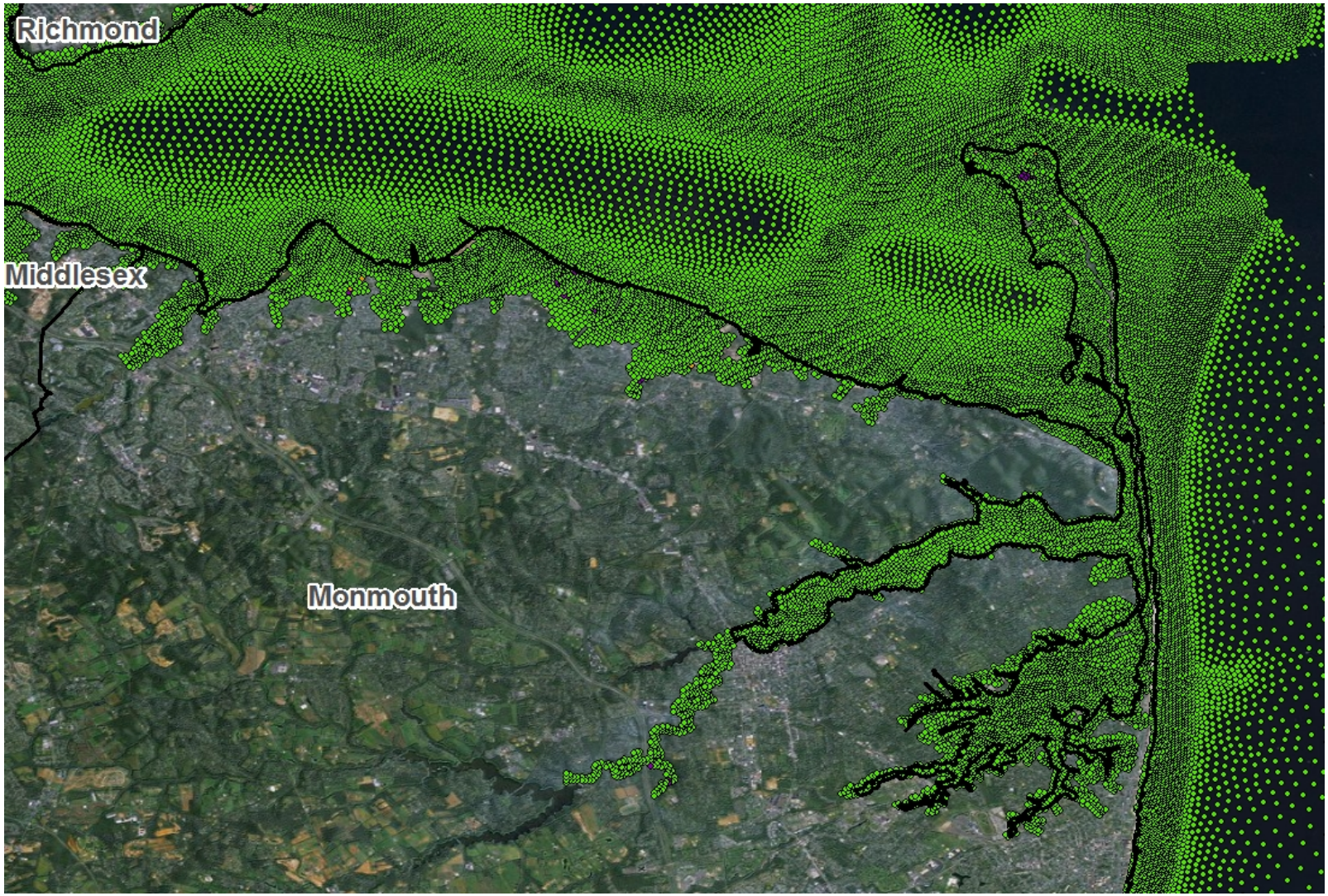

Figure B-6. Differences in 1%-annual-chance SWEL when comparing updated results from sensitivity testing (37 storms) to original results.

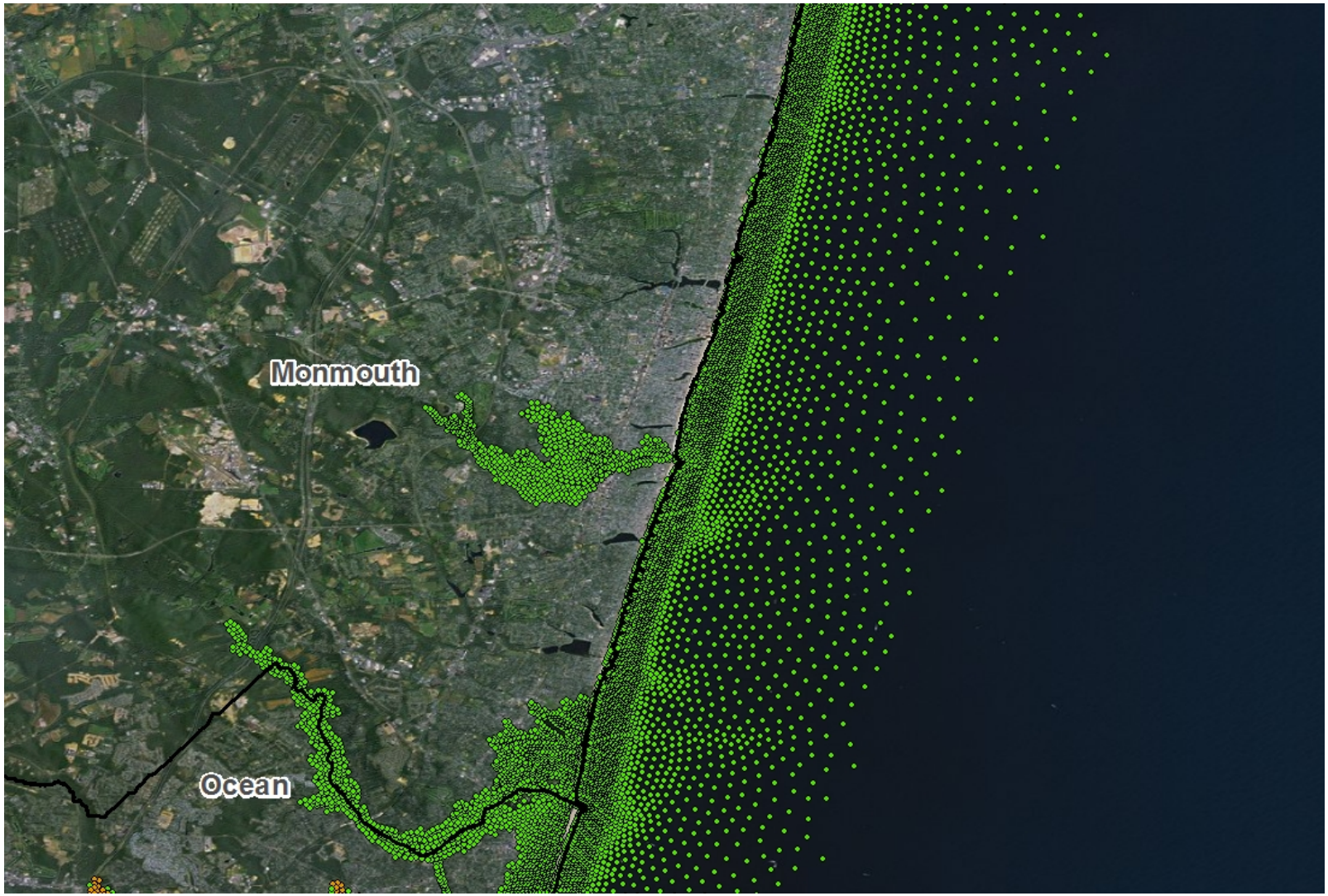

Figure B-7. Differences in 1%-annual-chance SWEL when comparing updated results from sensitivity testing (37 storms) to original results.

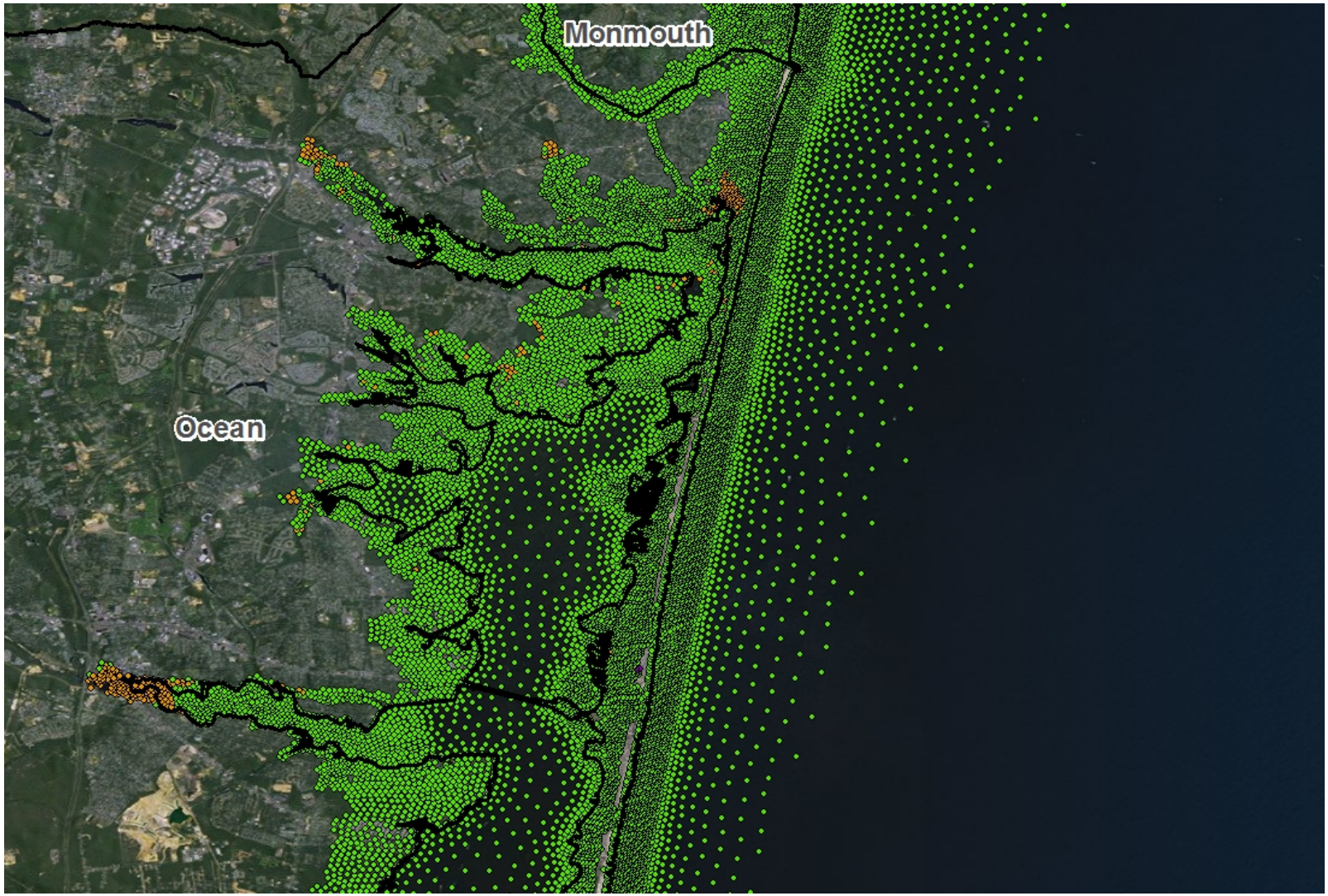

Figure B-8. Differences in 1%-annual-chance SWEL when comparing updated results from sensitivity testing (37 storms) to original results.

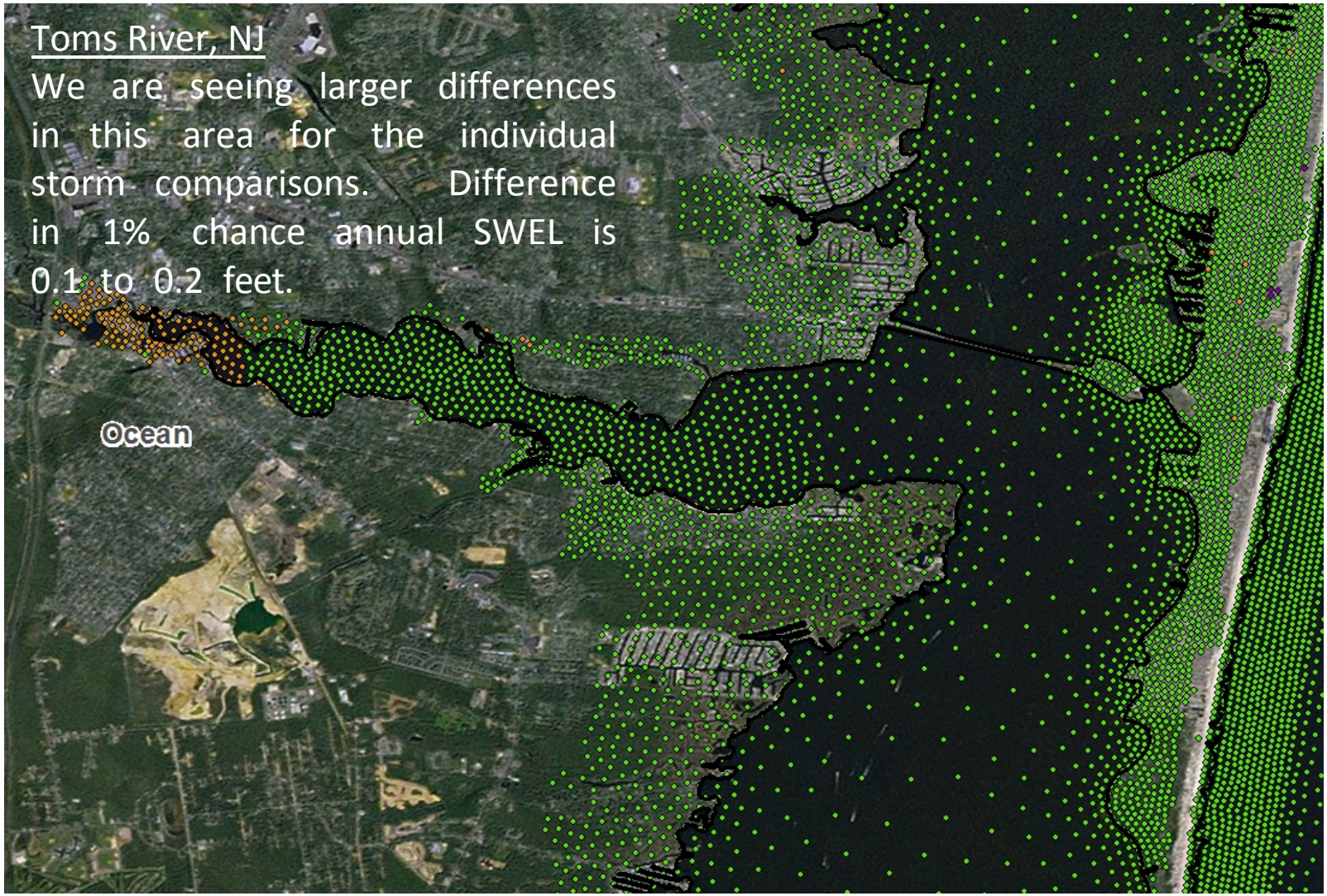

Figure B-9. Differences in 1%-annual-chance SWEL when comparing updated results from sensitivity testing (37 storms) to original results.

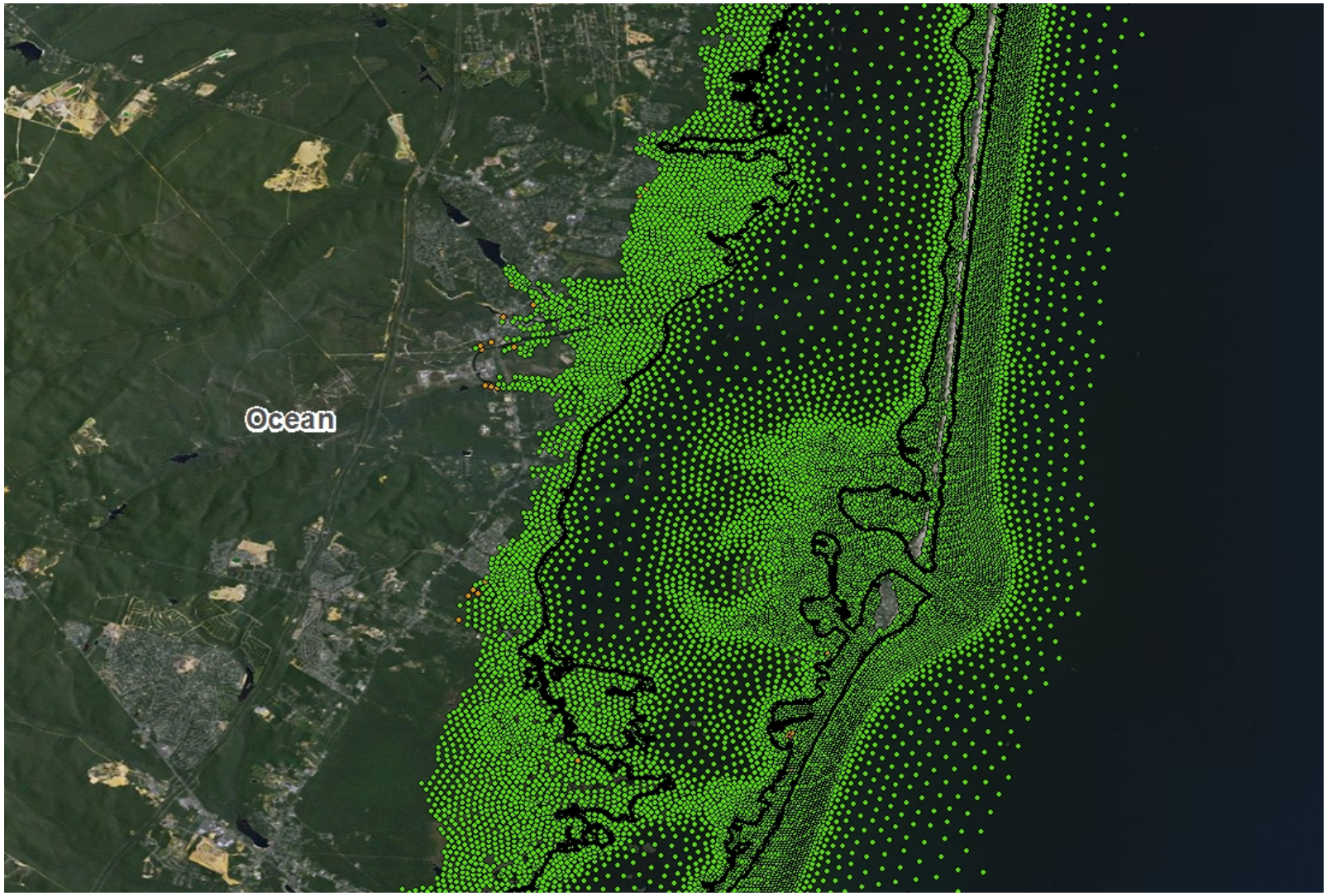

Figure B-10. Differences in 1%-annual-chance SWEL when comparing updated results from sensitivity testing (37 storms) to original results.

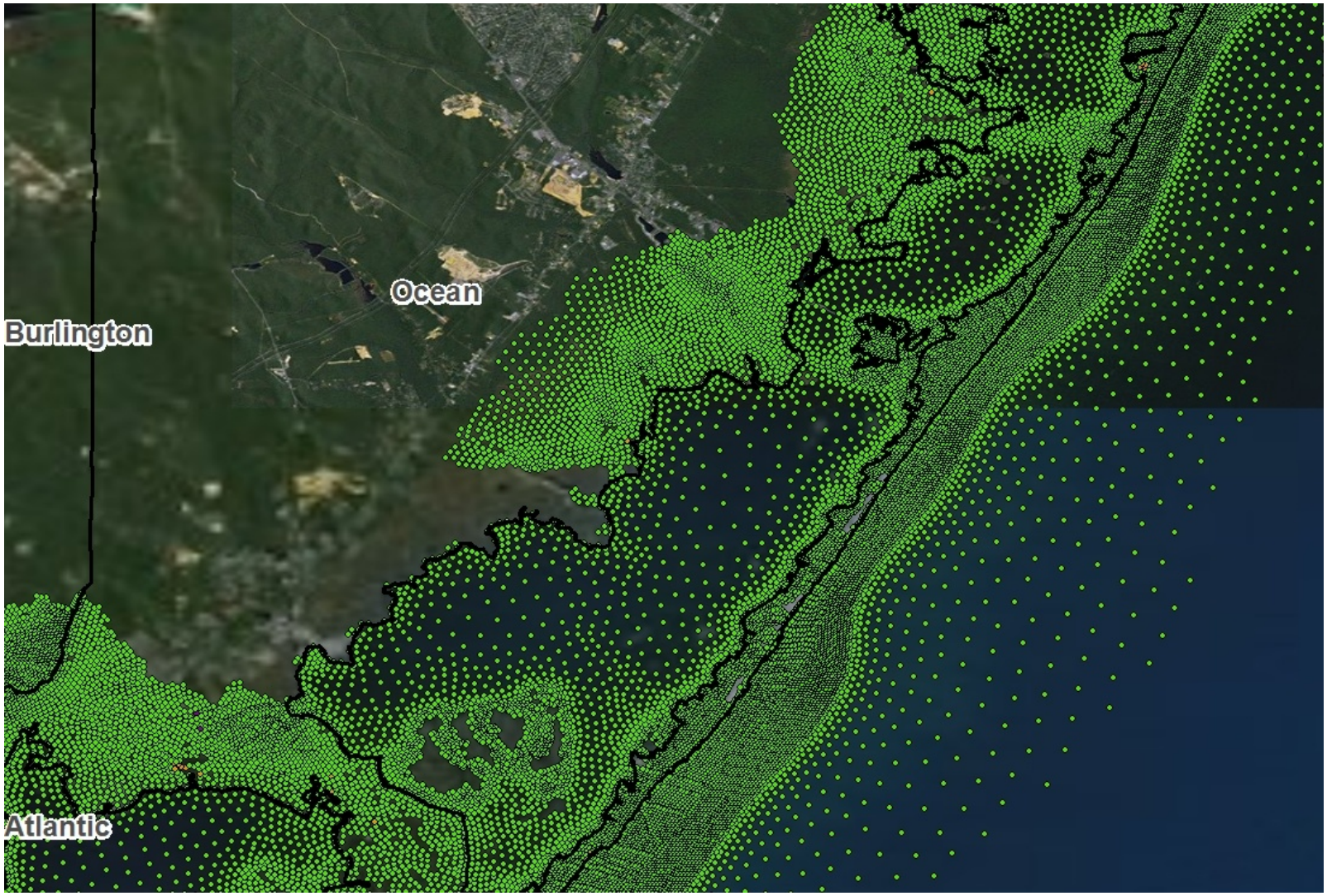

Figure B-11. Differences in 1%-annual-chance SWEL when comparing updated results from sensitivity testing (37 storms) to original results.

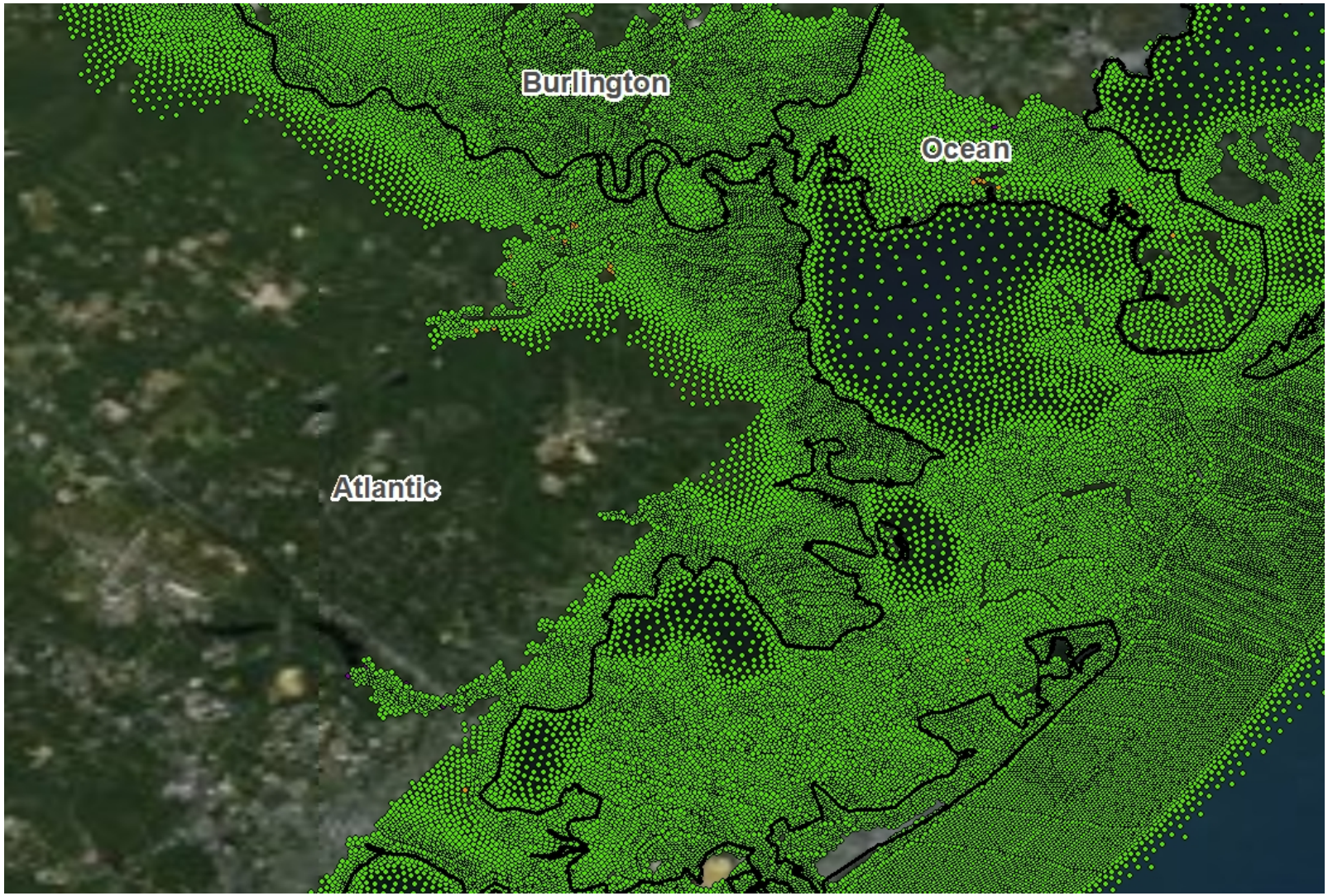

Figure B-12. Differences in 1%-annual-chance SWEL when comparing updated results from sensitivity testing (37 storms) to original results.

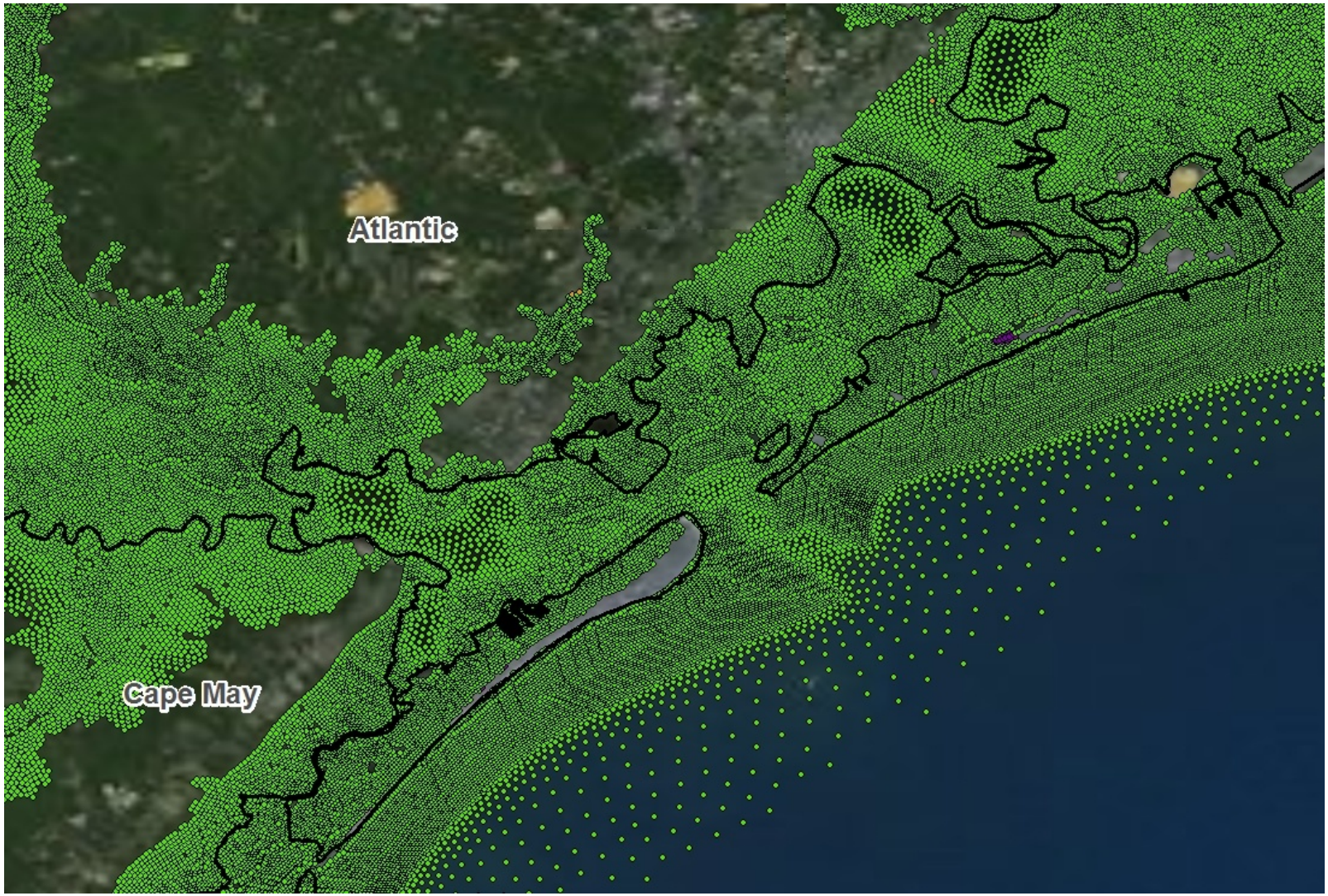

Figure B-13. Differences in 1%-annual-chance SWEL when comparing updated results from sensitivity testing (37 storms) to original results.

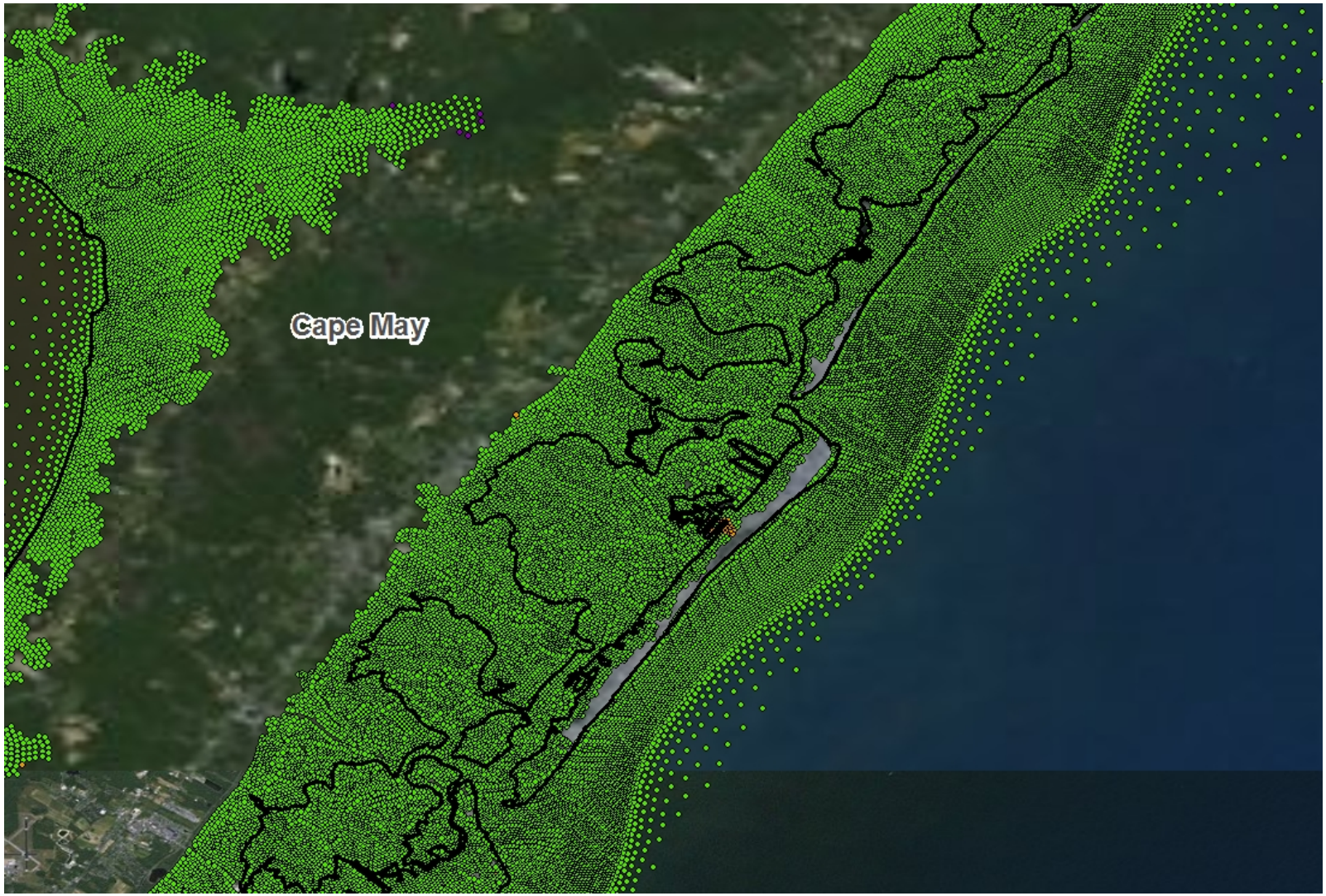

Figure B-14. Differences in 1%-annual-chance SWEL when comparing updated results from sensitivity testing (37 storms) to original results.

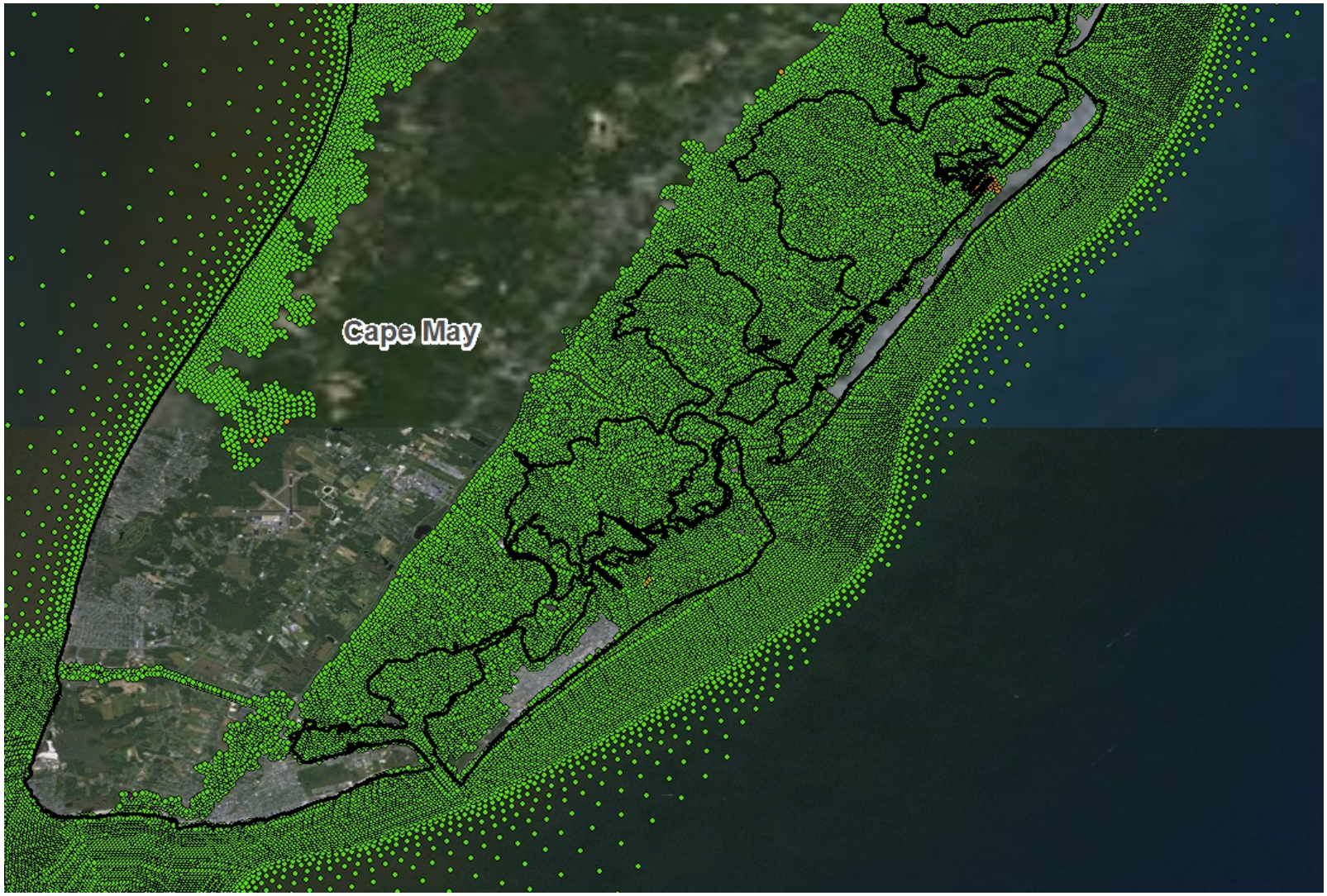

Figure B-15. Differences in 1%-annual-chance SWEL when comparing updated results from sensitivity testing (37 storms) to original results.